Geoderma 460 (2025) 117408

Contents lists available at ScienceDirect

Geoderma

journal homepage: www.elsevier.com/locate/geoderma

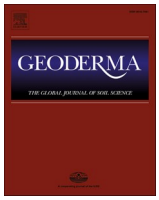

Microbial biomass – not diversity – drives soil carbon and nitrogen mineralization in Spanish holm oak ecosystems

Elisa Bruni [a,*], Jorge Curiel Yuste [b,c], Lorenzo Menichetti [d], Omar Flores [e], Daniela Guasconi [f], Bertrand Guenet [a], Ana-Maria Hereș [g], Aleksi Lehtonen [d], Raisa Mäkipää [d], Marleen Pallandt [f], Leticia Pérez-Izquierdo [b], Etienne Richy [h], Mathieu Santonja [i], Boris Tupek [d], Stefano Manzoni [f]

[a] Laboratoire de Géologie, Ecole Normale Supérieure, CNRS UMR 8538, Institut Pierre-Simon Laplace, PSL Research University, Paris, France
[b] BC3—Basque Centre for Climate Change, Scientific Campus of the University of the Basque Country, Leioa, Spain
[c] IKERBASQUE – Basque Foundation for Science, Plaza Euskadi 5, E-48009 Bilbao, Bizkaia, Spain
[d] Natural Resources Institute Finland (Luke), Latokartanonkaari 9, 00790 Helsinki, Finland
[e] Earth Sciences, Vrije Universiteit Amsterdam, Amsterdam, The Netherlands
[f] Department of Physical Geography and Bolin Centre for Climate Research, Stockholm University, Stockholm, Sweden
[g] Department of Forest Engineering, Forest Management Planning and Terrestrial Measurements, Faculty of Silviculture and Forest Engineering, Transilvania University of Brașov, Sirul Beethoven -1, 500123 Brașov, Romania
[h] Laboratory of Environmental Microbiology, Institute of Microbiology of the Czech Academy of Sciences, Prague 4, Czech Republic
[i] Aix Marseille Univ, Avignon Univ, CNRS, IRD, IMBE, Marseille, France

ARTICLE INFO

Handling Editor: Dr Cornelia Rumpel

Keywords:
Biogeochemistry
Modeling
Climate change
Microorganisms
Biodiversity
Forest soil

ABSTRACT

Soil microbial communities drive essential ecosystem functions, catalyzing biogeochemical cycles and contributing to climate regulation. However, due to the complexity of microbial communities, the magnitude and direction of microbial biomass and diversity contributions to carbon (C) and nutrient cycling remain unclear. For this reason, most models predicting soil organic matter (SOM) dynamics at the ecosystem level do not explicitly describe the role of microorganisms as mediators of SOM decomposition. Incorporating microbial properties, and especially diversity, into ecosystem models remains an open question, requiring careful consideration of the tradeoff between model complexity and performance.

This work addresses this knowledge gap by implementing a simple C and nitrogen (N) cycling model to predict heterotrophic respiration and net N mineralization rates in soils sampled under different land-uses and tree health conditions across Spain. To understand the role of microorganisms on ecosystem functioning, we progressively incorporated microbial biomass and diversity (i.e., alpha diversity of taxa and of fungal functional groups), and selected the model that optimized prediction accuracy, while minimizing complexity.

We found that microbial biomass had a strong and positive effect on both C and N mineralization rates, with heterotrophic respiration being nearly linearly controlled by biomass. In contrast, microbial diversity had minimal but negative effects on mineralization processes, with land-use differences explaining part of the variability in these effects. Our study confirms microbial biomass as a key driver of C and N mineralization rates, while highlights that microbial diversity based on taxonomic identification inadequately explains microbial effects on these ecosystem functions.

1. Introduction

Soil microbial communities are one of the most important biotic components of terrestrial ecosystems, contributing significantly to nutrient stock formation (Bird et al., 2008; Rubino et al., 2010; Mambelli et al., 2011; Cotrufo et al., 2013) and overall ecosystem diversity (Domeignoz-Horta et al., 2024). These communities drive essential ecosystem functions, ensuring plant residue decomposition, nutrient recycling, and soil organic matter (SOM) formation (Paul, 2007; Tate, 2017; Manzoni et al., 2010), and supporting plant health by enhancing

* Corresponding author.
E-mail address: bruni@geologie.ens.fr (E. Bruni).

https://doi.org/10.1016/j.geoderma.2025.117408
Received 3 February 2025; Received in revised form 27 April 2025; Accepted 18 June 2025
Available online 25 June 2025

nutrient availability and soil structure, e.g., via aggregate stabilization and particle transport (Bever et al., 2012; Sahu et al., 2019). Despite extensive research in recent decades, the quantitative effect of microbial communities on soil and ecosystem functioning is not clear yet (Graham et al., 2014, 2016; Martiny et al., 2015; Hall et al., 2018; Crowther et al., 2019). As a result, there is little consensus on how to integrate soil microbial attributes into models predicting terrestrial ecosystem responses to climate change (Lennon et al., 2024). Some soil carbon (C) cycling models have explicitly incorporated soil microbial biomass in their equations (e.g., Sulman et al., 2014; Wieder et al., 2014; Wang et al., 2015; Abramoff et al., 2017, 2018; Robertson et al., 2019; Zhang et al., 2021; Berardi et al., 2024). Typically, this is done using nonlinear kinetics to represent C transfers among compartments, although this approach inevitably increases model complexity and uncertainty in the predictions (Shi et al., 2018). In contrast, microbial community composition and diversity have been less frequently integrated into such models due to the greater complexity of microbial diversity itself (Louis et al., 2016). Though some examples exist (e.g., Wieder et al., 2014; Zhang et al., 2021), incorporating diversity via a mechanistic representation of processes may not always be desirable when the objective is to improve model accuracy at large scales. For the past few decades, the prevailing paradigm has emphasized the functional and biological redundancy of soil microorganisms (Nannipieri et al., 2017). Yet, emerging evidence suggests that microbial properties, such as species diversity, can be robust predictors of SOC (Wang et al., 2023) and SOC decomposition rates (Domeignoz-Horta et al., 2020), with microbial diversity also proposed as a means to enhance model accuracy (Louis et al., 2016). Nevertheless, many of the models developed over the years have not been validated against empirical data (Louis et al., 2016). Consequently, the role of microbial diversity in predicting terrestrial ecosystem processes remains largely untested at large scales (Lennon et al., 2024). To address this gap, it is essential to agree on whether the integration of biomass and diversity of soil microbial communities improves the accuracy of predictive models. Establishing general patterns that define their role in ecosystem functioning will refine our understanding of how terrestrial ecosystems will respond to future environmental challenges.

Soil microbial biomass affects the C balance through two main mechanisms. First, it promotes plant litter and SOM decomposition, contributing to C loss via heterotrophic respiration (Berg and McClaugherty, 2020). Second, microbial product formation can be stabilized through organo-mineral interactions (e.g., adsorption and complexation) or aggregation, contributing significantly to SOM accumulation (Cotrufo et al., 2013; Gleixner, 2013; Kallenbach et al., 2016; Malik et al., 2018; Bastida et al., 2021). Most models predicting SOM dynamics at the ecosystem level do not explicitly describe the role of microorganisms as mediators of C and nutrient decomposition, but consider decomposition as dependent only on the amount and quality of soil substrates and on pedo-climatic conditions (Manzoni and Porporato, 2009; Le Noë et al., 2023). These models, based on first-order kinetic exchanges, are considered to capture the essential C and nutrient dynamics (e.g., Coleman and Jenkinson, 1996; Parton et al., 1988). However, by neglecting the pivotal effect of microbial biomass on SOM evolution and its capacity to decompose specific substrates, they lack the mechanisms to predict SOM responses to global change (Todd-Brown et al., 2014; Mäkipää, 2023). For example, it remains uncertain how climate and land-use changes will affect the rates of biogeochemical processes regulated by microbial activity and biomass (Cavicchioli et al., 2019).

Microbial diversity also contributes significantly to explaining soil functions (Graham et al., 2016). Generally, diversity — as measured by taxonomic richness — affects biogeochemical rates, including decomposition rates of SOM (Valentin et al., 2014) and heterotrophic respiration (Setälä and McLean, 2004; Bell et al., 2005; Wilkinson et al., 2012; Domeignoz-Horta et al., 2020). While most studies report positive effects on these rates (Setälä and McLean, 2004; Bell et al., 2005; Wilkinson et al., 2012; Domeignoz-Horta et al., 2020), others report weak or even negative effects, or different effects depending on the substrate being decomposed (Tiunov and Scheu, 2005). A caveat of many of these studies is that they were conducted under idealized conditions with low-diversity manipulated microbial communities. Yet, they point to mutualistic effects that would be expected in high-diversity natural communities as well. Other studies based on field data at larger scales likewise suggest that increased microbial diversity is positively associated with soil functioning in terrestrial ecosystems (Delgado-Baquerizo et al., 2016; Delgado-Baquerizo et al., 2017). Mathematical models also predict higher biogeochemical rates with increasing microbial diversity, aligning with most of the experimental studies (Loreau, 2001; Khurana et al., 2023). However, most of the models currently used to predict soil organic carbon (SOC) and nitrogen (N) dynamics at the ecosystem level do not account for microbial diversity yet. While we expect diversity to be relevant at the ecosystem level (Graham et al., 2016), it remains unclear whether incorporating it would improve model predictions.

Additionally, little is known about microbial diversity effect on N mineralization rates, which are fundamental for plant nutrition. Some evidence points to a positive effect of diversity on net N mineralization (Setälä and McLean, 2004), which would be expected due to the positive relation between OM decomposition rates and net N mineralization (Setälä and McLean, 2004). However, N mineralization is influenced not only by microbial metabolic capacity but also by their stoichiometric requirements, adding another layer of complexity to how microbial diversity affects the N cycle. Whether N is released or immobilized by the microbial biomass depends primarily on the balance between the microbial demand for N (required for growth) and the supply of N from the decomposing substrates (Manzoni et al., 2010). This balance can be described by the so-called ‘critical C:N’ or ‘threshold element ratio’ (TER), above which substrates are too N-poor to allow for a net N release to occur (Sterner and Elser, 2002). The TER is defined as the ratio between microbial C:N ratio and microbial C use efficiency (CUE), and both of these microbial traits depend on microbial community composition. CUE tends to decrease as the ratio between fungal and bacterial growth rates increases (Soares et al., 2017) and is sensitive to changes in microbial diversity—in some cases increasing (Domeignoz-Horta et al., 2020), and in others decreasing with increasing diversity (Maynard et al., 2017). Microbial C:N is higher in fungi than in bacteria, although at the whole community level, variations in microbial C:N tend to be minor across ecosystems (Xu et al., 2013). As a result, we would expect microbial community composition and possibly diversity to modulate not only C, but also N mineralization rates through their effects on microbial traits determining the microbial N demand.

In this contribution, we evaluate a simple C and N cycling model that incorporates microbial biomass and diversity metrics to predict heterotrophic respiration and net N mineralization rates. Using a dataset from 18 holm oak-dominated sites across Spain (García-Angulo et al., 2020), we explore the effects of microbial biomass and diversity under a wide range of soil types, land-uses, and forest health conditions. This dataset offers a unique opportunity to assess the role of microbial communities in regulating heterotrophic respiration and net N mineralization across a representative sample of regional conditions (i.e., the Spanish Iberian Peninsula). The model features minimal complexity, allowing key kinetic and stoichiometric parameters to be calibrated against observational data. We progressively incorporate microbial biomass and diversity (defined in several different ways) into the model, identifying the most parsimonious model variant for predicting observed C and N mineralization rates. We hypothesize that both microbial biomass and diversity positively affect heterotrophic respiration and net N mineralization rates, thereby improving model predictions compared to models that neglect biomass and diversity effects.

2. Materials and methods

2.1. Experimental sites

We used data from an experimental study that aimed to determine the effect of holm oak (*Quercus ilex* L. subsp. *ballota* [Desf.] Samp) decline on soil processes (García-Angulo et al., 2020). In addition to the data from García-Angulo et al. (2020), our dataset includes five additional holm oak sites that were not part of the original publication but were sampled and analyzed by the same authors using the exact same design and procedures (Fig. 1). In total, we used data from 18 sites across Spain (Fig. 1), spanning wide climatic conditions and soil pH gradients. Mean annual temperature ranged between 10 °C and 16 °C and mean annual precipitation between 282 mm and 916 mm, while soil pH ranged from very acidic (5.1) to alkaline (7.9). The study sites were under different land-uses, namely forests, open woodlands, and dehesas (i.e., savannah-like ecosystems, Pulido et al., 2001; Herguido Sevillano et al., 2017). Soil organic matter C:N ratio ranged between 4.9 and 24.8, and soil organic C and microbial biomass C contents varied widely across sites (from 10 g C kg^{-1} to 187 g C kg^{-1} and from 0.7 g C kg^{-1} to 6.6 g C kg^{-1}, respectively) (García-Angulo et al., 2020).

In our analyses (described in Sections 2.5–2.9), we used site-specific measurements of soil organic C content, biomass C content, microbial diversity, and organic matter C:N ratio to fit our models, while also allowing land-use to modulate model parameters. Other site characteristics were assumed to be captured indirectly through these variables, as well as land-use. As soils were incubated in controlled conditions, climate per se is expected to have only an indirect effect via those proxies.

2.2. Soil sampling

Here, we report the main methods used by García-Angulo et al. (2020) to obtain soil samples, and further details can be found in their publication. To uniformly cover the area and account for within-site heterogeneity, three subplots were established at each of the 18 sites. Each subplot included 9 holm oak trees, representing three crown defoliation levels – healthy, affected, and dead – with three trees per condition to capture the range of ecosystem variability. The five additional sites of this study (i.e., Almería, Arascués, Léon, Navas de Estena, and Sevilla-Usera) included only three holm oak trees per subplot because only healthy trees were present and thus sampled (i.e., no crown defoliation was observed at these sites). To account for spatial heterogeneity, three soil samples were collected at 0–10 cm depth beneath each tree canopy, within a 50 cm radius of the trunk, and pooled together into a composite soil sample. For each crown defoliation level, three additional soil samples were obtained from outside the tree canopy and similarly pooled into a composite soil sample. This resulted in 12 composite soil samples per site at the 13 locations with crown defoliation variation (i.e., 156 soil samples) and 6 composite samples per site at the 5 locations with only healthy trees (i.e., 30 soil samples). Therefore, this study has been carried out with a total of 186 composite soil samples.

All soil samples were extracted with a 5 cm diameter metallic cylinder from the first 10 cm of the soil after leaf litter (OL layer) removal. Hence, the samples contained both a part of the organic horizon and a part of the A horizon of the mineral soil. Soil samples were immediately stored in a portable fridge at constant 4 °C temperature until arrival to the laboratory. Upon arrival, soil within each bag was homogenized prior to manipulation. An aliquot of approx. 15 g was separated from each of the 186 composite soil samples and frozen for subsequent soil microbial diversity analysis. The remaining soil was dried at room temperature (for approx. 15 days), sieved using a 2 mm mesh size, and stored in a dry dark place until further analyses. For all soils, physico-chemical analyses were also performed on dry soil samples, namely to measure soil organic C, total soil N, bulk density, and pH (see García-Angulo et al. (2020)).

2.3. Measurements of heterotrophic respiration and net N mineralization

To measure microbial C and net N mineralization rates, 40 g of dry soil were placed in a 150 mL glass jar and rehydrated to reach 40 % of the soil water holding capacity (WHC). In order to avoid potential non-linear increases in CO_2 production after rewetting (Birch, 1958), soils were incubated for 48 h after rewetting while their water content was kept constant. Soil samples were then incubated for 15 days following a temperature response curve ranging from 5 °C to 35 °C. Microbial C and N mineralization rates were measured at every 10 °C increment (i.e., at 5 °C, 15 °C, 25 °C, and 35 °C), and the values used in this study represent the average values across these temperatures. In particular, microbial C mineralization was measured as soil heterotrophic CO_2 production (i.e., heterotrophic respiration, R), and net N mineralization (M) was measured as the change over time (between day 15 and day 0 of the soil incubation period) in soil mineral N concentration (defined as the sum of NO_3^- –N and NH_4^+ –N). For more information about the methodology used to measure C and N mineralization rates, see García-Angulo et al.

Fig. 1. Location of field sites in the Spanish Iberian Peninsula; different colors and shapes indicate the land-use at each site (modified after García-Angulo et al. (2020)).

(2020).

2.4. Microbial biomass and diversity

Soil microbial biomass (including both fungi and bacteria) was measured using a substrate-induced respiration (SIR) method (Anderson and Domsch, 1978), modified according to García-Angulo et al. (2020). This widely-used method consists in estimating the living soil microbial biomass by measuring the maximum respiratory response of the microbial community in the soil samples after adding an excess of C and energy source, such as glucose. The addition of available C at saturation concentrations triggers a strong increase in the respiration rate (five- to ten-fold), known as substrate-induced respiration. This response reflects the biomass of microorganisms capable of rapidly utilizing the substrate (Anderson and Domsch, 1978), representing the active or potentially active fraction of the soil microbial community, which is a significant fraction of the total microbial biomass (Blagodatskaya and Kuzyakov, 2013). The SIR method is considered a robust approach for assessing living microbial biomass and has been extensively compared to other methodologies such as fumigation-extraction (e.g., Cheng and Virginia, 1993; Harden et al., 1993). To perform SRI, a subsample of 10 g of dry soil was placed in a glass jar, and rehydrated to 40 % of its WHC. Afterwards, a 0.5 g glucose kg^{-1} of dried soil was added and the soil was incubated for two hours at 30 °C. After the incubation, CO_2 emissions were measured using a portable soil gas exchange system (EGM-4, PP systems, MA, USA). For more information see García-Angulo et al. (2020).

To assess microbial diversity, DNA was extracted from frozen soil aliquots that were immediately separated after sampling. DNA was amplified targeting the ITS1 region and the V4–V5 regions of the 16S rRNA gene and sequenced using Illumina MiSeq v2 to identify fungal and bacterial taxa, respectively. The sequences were processed with Qiime v1.9.1 (Caporaso et al., 2010), which identifies and removes chimeras through USEARCH v6.1 (Edgar, 2010) by using the RDP gold database for bacteria (Cole et al., 2014) and the UNITE chimera database for fungi (Nilsson et al., 2019). The resulting sequences were grouped into operational taxonomic units (OTUs) and identified with an open-reference OTU picking process (pick_open_reference_otus from Qiime v1.9.1) at a 97 % sequence identity to taxonomically assign the representative sequences for each OTU. For this, the RDP classifier database (i.e., with a threshold of 0.8) was used as a reference for bacteria. The process of clustering the fungal ITS sequences was similar to that used for bacteria but, in this case, the taxonomic identification of representative OTUs was made using the UNITE database as a reference. More details on these procedures can be found in García-Angulo et al. (2020). In our study, we performed new analyses as follows. We used the FungalTraits database to further identify saprotrophic and ectomycorrhizal fungi (Põlme et al., 2021). After removing singletons, the fungal and bacterial datasets were rarefied to 3520 and to 8159 counts, respectively, using the SRS package (Beule and Karlovsky, 2020). The resulting rarefied libraries were used to calculate alpha diversity indices using the *phyloseq* package in R (McMurdie and Holmes, 2013). In addition to OTU richness (S), we calculated the Shannon-Weiner index (H; hereinafter referred to as Shannon) and the inverse Simpson index (IS) for all fungi and bacteria, as well as for the major fungal functional groups i.e., saprotrophic and ectomycorrhizal fungi (Fig. 2.1). For each of the alpha diversity indices, we also calculated a combined index accounting for both bacterial and fungal diversity as,

$$f_0 = \sqrt{f_{0,fungi}\ f_{0,bacteria}} \tag{1}$$

where $f_{0,fungi}$ and $f_{0,bacteria}$ are fungal and bacterial diversity indices, respectively (i.e., fungal and bacterial richness, S, Shannon-Weiner index, H, and Inverse Simpson index, IS, Table S1). All these diversity indices were used to build 32 different models of C and N dynamics accounting for microbial diversity (Fig. 2.2).

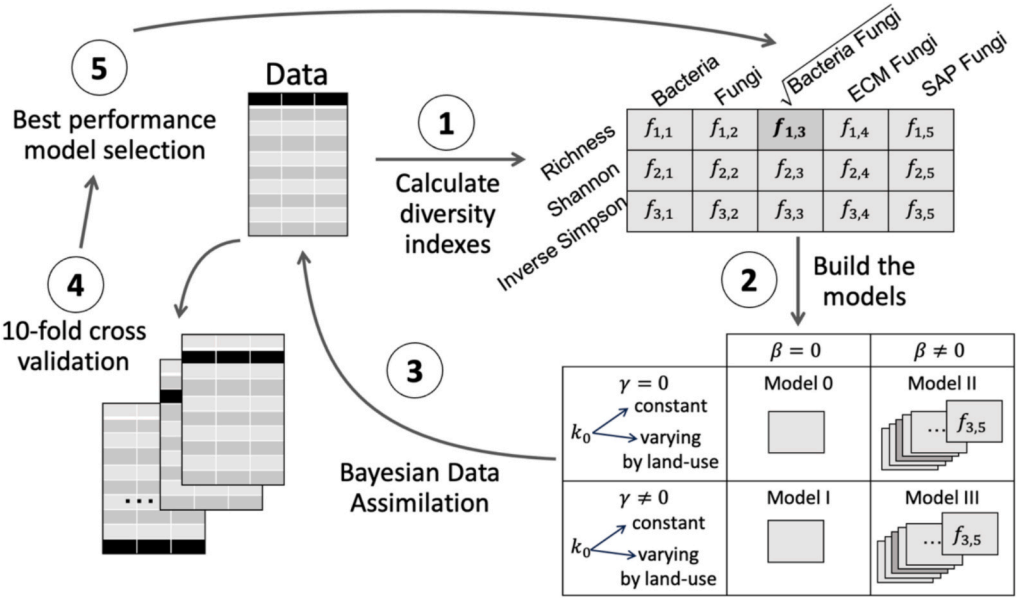

Fig. 2. Illustration of the 5-step process for model selection based on diversity indices and Bayesian data assimilation: (1) Raw data (i.e., microbial functional groups such as bacteria, fungi, combined fungi and bacteria, ectomycorrhizal (ECM) fungi, and saprotrophic (SAP) fungi) are used to compute various diversity indices (i.e., Richness, Shannon, and Inverse Simpson), resulting in a total of 15 microbial diversity indices; (2) different models are constructed based on varying assumptions about the influence of microbial biomass ($\gamma \neq 0$ in Eq. (2)) and microbial diversity ($\beta \neq 0$ Eq. (6)) on heterotrophic respiration and net N mineralization rates. Models including the effect of microbial diversity (i.e., models II and III) were built for each of the 15 diversity indices (denoted here $f_{i,j}$, with i = 1, …, 3 and j = 1, …, 5), resulting in a total of 32 models; (3) model parameter probability distributions are estimated via a Bayesian data assimilation framework to predict heterotrophic respiration and net N mineralization. Two calibration strategies are carried out, one with constant decay rate coefficient k_0, and one with k_0 varying by land-use; (4) the models undergo a 10-fold cross-validation, where the dataset is split into 10 subsets and the models' performance is tested iteratively on the different subsets; (5) finally, the best performance models are selected based on the average cross-validation results.

2.5. Exploratory data analysis

An exploratory data analysis was conducted to assess differences in microbial biomass and diversity across the different land-use types, with a special focus on bacterial and fungal richness. After testing for normality of the variables with Shapiro test (Royston, 1982) and homoscedasticity with Levene test (Levene, 1960), we assessed statistical differences between land-use types using analysis of variance (ANOVA) followed by post-hoc Tukey pairwise tests (Miller, 1981), or alternative non-parametric tests (i.e., Kruskal-Wallis test followed by post-hoc Wilcoxon pairwise test, Hollander and Wolfe (1973)) when these assumptions were not met (i.e., for microbial biomass and bacterial richness).

2.6. Model of heterotrophic respiration and net N mineralization

We considered a simple model of soil C and N dynamics, where we could define microbial growth, heterotrophic respiration, uptake, and net N mineralization (symbols are defined in Table 1). This model can be adjusted by including modifier functions to account for the roles of microbial biomass and diversity on heterotrophic respiration and net N mineralization. These functions can be turned on or off, and by comparing the predictive power of each resulting model, we can assess the impact of these variables on soil functions. The model is based on the partitioning of organic C and N taken up by microorganisms into new biomass and mineralization products: CO_2 from the respiration of organic C, and inorganic N released from the metabolism of organic N. We do not consider nitrification, denitrification, and dissimilatory nitrate reduction to ammonium, which are important processes in the N cycle, but fall outside the scope of this study.

Table 1
Explanations and units of symbols used in the equations for the C and N cycling model.

Symbol	Explanation	Units	Sources
C_B	Soil microbial biomass C content	gC kg^{-1}	Measured
C_S	Soil organic C content	gC kg^{-1}	Measured
$(C:N)_B$	Microbial biomass C:N ratio	gC gN^{-1}	Xu et al. (2013)
$(C:N)_S$	Soil organic matter C:N ratio ($(C:N)_S = C_S/N_S$)	gC gN^{-1}	Measured
CUE	Microbial C use efficiency (CUE = G/U)	–	Calibrated
f_0	Microbial functional diversity	–	Calculated from OTUs
G	Microbial growth rate	gC kg^{-1} d^{-1}	Calculated
H	Shannon-Weiner diversity index	–	Calculated from OTUs
IS	Inverse Simpson diversity index	–	Calculated from OTUs
k_0	Rate constant for diversity	d^{-1} for $\gamma = 0$ $\left(gC\,kg^{-1}\right)^{-\gamma} d^{-1}$ for $\gamma \neq 0$	Calibrated
k_R	Rate constant for heterotrophic respiration ($k_R = (1-CUE)k_U$)	d^{-1} for $\gamma = 0$ $\left(gC\,kg^{-1}\right)^{-\gamma} d^{-1}$ for $\gamma \neq 0$	Calculated
k_U	Rate modifier for C uptake or decomposition	d^{-1} for $\gamma = 0$ $\left(gC\,kg^{-1}\right)^{-\gamma} d^{-1}$ for $\gamma \neq 0$	Calculated
M	Net N mineralization rate	gN kg^{-1} d^{-1}	Calculated and measured
N_S	Soil organic N content	gN kg^{-1}	Measured
R	Heterotrophic respiration rate	gC kg^{-1} d^{-1}	Calculated and measured
S	Microbial richness (number of OTUs)	–	Measured
TER	Threshold element ratio ($TER = (C:N)_B/CUE$)	gC gN^{-1}	Calculated
U	Microbial C uptake rate	gC kg^{-1} d^{-1}	Calculated
β	Exponent for microbial diversity effects	–	Calibrated
γ	Exponent for C_B in the microbial uptake kinetics	–	Calibrated

Mathematically, it is convenient to start by defining the microbial uptake rate (U),

$$U = k_U C_S C_B^{\gamma} \tag{2}$$

where k_U is the decay rate for C uptake, C_S is the organic C content in the soil, C_B is the microbial biomass C content, and γ is an exponent representing the effect of microbial biomass on the uptake rate. With $\gamma = 0$, Eq. (2) becomes a classical first order decay model where SOC is decomposed at a constant k_U rate, while $\gamma = 1$ leads to a multiplicative model in which uptake depends linearly on both organic C content and microbial biomass (Manzoni and Porporato, 2007). With this model ($\gamma = 1$), biomass specific respiration (i.e., metabolic quotient) scales linearly with organic C content. It should also be noted that the rate of microbial uptake is equal to the rate of decomposition, because we do not model the dynamics of depolymerization products. Other kinetics can be more appropriate under varying environmental conditions or when microbial biomass changes during the incubation (e.g., Tang and Riley, 2017). However, in the case study considered here incubation conditions are controlled and the duration is short, so that the simple kinetics in Eq. (2) are a reasonable approximation.

Microbial growth (G) is described as the product of C use efficiency (CUE) and organic C uptake rate, $G = CUE\ U$ (Manzoni and Porporato, 2009). Accordingly, heterotrophic respiration (R) is defined as,

$$R = U - G = (1 - CUE)U = (1 - CUE)k_U C_S C_B^{\gamma} = k_R C_S C_B^{\gamma} \tag{3}$$

where in the last equality we defined the rate constant for respiration as $k_R = (1 - CUE)k_U$.

Net N mineralization (M) can be calculated as the difference between microbial N supply from organic matter decomposition and microbial N demand for growth (Manzoni and Porporato, 2009),

$$M = \underbrace{U\frac{N_S}{C_S}}_{N\ \ uptake} - \underbrace{\frac{G}{(C:N)_B}}_{N\ \ demand} = U\left[\frac{1}{(C:N)_S} - \frac{CUE}{(C:N)_B}\right] \tag{4}$$

where N_S is the content of organic N, and $(C:N)_B$ and $(C:N)_S$ are the C:N ratios of microbial biomass and organic matter, respectively. The last expression on the right-hand side of Eq. (4) is the result of minor rearrangements and a more compact notation. When substrate C:N ratio is low, net N release occurs ($\frac{1}{(C:N)_S} > \frac{CUE}{(C:N)_B}$), whereas net N immobilization occurs when substrate C:N is high, requiring acquisition of mineral N from the soil environment to compensate for the microbial stoichiometric imbalance ($\frac{1}{(C:N)_S} < \frac{CUE}{(C:N)_B}$). The threshold C:N ratio at which net N mineralization is exactly zero ($\frac{1}{(C:N)_S} = \frac{CUE}{(C:N)_B}$) is referred to as the 'threshold element ratio' (TER) (Sterner and Elser, 2002), i.e., $TER = \frac{(C:N)_B}{CUE}$. Higher values of microbial C:N or lower values of CUE increase the TER, ensuring net N release even if substrates are N poor (Manzoni et al., 2010).

Usually, heterotrophic respiration rates are measured instead of uptake rates. Therefore, Eq. (4) can be expressed as follows, recalling that $R = (1 - CUE)U$,

$$M = \frac{R}{1 - CUE}\left[\frac{1}{(C:N)_S} - \frac{CUE}{(C:N)_B}\right] \tag{5}$$

In this framework, any microbial diversity effect altering the value of the kinetic constant k_R or possibly the other parameters (γ, CUE, $(C:N)_B$) would affect the heterotrophic respiration (Eq. (4)) and N mineralization rates (Eq. (5)).

It is important to emphasize that despite its simplicity, this model of heterotrophic respiration and net N mineralization is representative of

the kinetics and stoichiometric constraints implemented in the majority of soil C and N cycling models (Manzoni and Porporato, 2009). Therefore, we would expect that results obtained from this minimal single-compartment model can be at least conceptually transferred to more complex multi-compartmental models such as those used in Bruni et al. (2022).

2.7. Effects of microbial diversity on C and N fluxes

To include the effect of microbial diversity in our model framework, we start by redefining the decay rate for C uptake (k_U) as an exponential with upper limit 1,

$$k_U = \min\{k_0 e^{\beta f_0}, 1\} \quad (6)$$

We refer here to a general microbial diversity index (f_0) (Fig. 2.1), to which is associated a decay coefficient (k_0) and a diversity coefficient (β). If $\beta = 0$, total decay rate equals k_0, and heterotrophic respiration and net N mineralization become insensitive to changes in diversity (Fig. S1). For values of $\beta > 0$, microbial diversity positively affects the heterotrophic respiration. In particular, when diversity (f_0) is low, the exponential term converges to 1 and the total decay rate approaches k_0, while for high diversity the decay rate for C uptake (k_U) is upper-bounded to 1 (Fig. S1). Values of $\beta < 0$ indicate negative effects of microbial diversity on heterotrophic respiration, with high diversity having maximum decomposition rate k_0, and low diversity having a decomposition rate approaching 0 (Fig. S1). Because net N mineralization depends on the respiration rate (Eq. (5)), any diversity effect in Eq. (4) will propagate from R to M.

Next (Fig. 2.3), we test four models based on Eqs. (3) and (5) (Table 2). Model 0 without the effects of microbial biomass or diversity ($\gamma = 0$ and $\beta = 0$); Model I where the effect of microbial biomass is considered, but not that of diversity ($\beta = 0$); Model II where only the effect of microbial diversity is considered ($\gamma = 0$); and finally Model III where both effects of biomass and diversity are considered (Table 2). Models with microbial diversity were tested with all diversity indices (Fig. 2.1) and results are shown for the diversity index based on fungal and bacterial richness combined according to Eq. (1). Results for all diversity indices are reported in the Supplementary Material (Table S1).

2.8. Model parameterization

Eqs. (3) and (5) can be constrained by observations of heterotrophic respiration and net N mineralization rates (R, M), of soil organic C and N contents (C_S, N_S, and their ratio $(C:N)_S$), and of microbial biomass C content (C_B). Parameters k_0, γ, and β, and in addition CUE and $(C:N)_B$ remain unconstrained as they were not measured by García-Angulo et al. (2020). Among these parameters, the C:N of microbial biomass is probably the least variable, so we set it at $(C:N)_B = 7$ g C g N^{-1} (based on average values for mixed and temperate forests from Xu et al., 2013). The remaining parameters k_0 and CUE, and the exponents γ and β are estimated through Bayesian data assimilation (Fig. 2.3). For that, we estimate the posterior distribution $P(\Theta|\boldsymbol{O})$ of the parameters (Θ) conditional to the observed data ($\boldsymbol{O}$) of heterotrophic respiration and net N mineralization, and based on prior knowledge on the parameters. Parameters were assumed to be uniformly distributed within their prior ranges, i.e., we selected an uninformative approach that assigns equal probability to all values within these realistic ranges due to limited prior knowledge (Table 4). Assuming that errors in the observed data followed Gaussian distributions, we constructed the likelihood function as,

$$P(\boldsymbol{O}|\Theta) = \prod_{i=1}^{N} \frac{1}{\sqrt{2\pi}\sigma} e^{-\frac{(Y_i(\Theta)-O_i)^2}{2\sigma^2}} \quad (7)$$

where Y_i are model predictions of heterotrophic respiration and net N mineralization, with $i = 1, \cdots N$, and $N = 124$ (i.e., 62 observations for each variable), O_i are observed heterotrophic respiration and net N mineralization for $i = 1, \cdots N$, and σ is the standard deviation of the distribution. The values of σ were also calibrated and the likelihood function was maximized to achieve the best agreement between model predictions and observations of heterotrophic respiration and net N mineralization rates.

Posterior probability distributions of the parameters were derived

Table 3
Average performance metrics of the 10-fold cross validation (Fig. 2.4) for the four model variants (0, I, II, and III, with constant k_0 across land-uses). For models II and III, only the results obtained using the diversity index of combined fungal and bacterial richness ($f_0 = \sqrt{S_{fungi} S_{bacteria}}$) are shown (Fig. 2.5). Model performance is evaluated using the coefficient of determination (R^2) and the root mean squared error (RMSE), calculated separately for heterotrophic respiration (R) and net N mineralization (M) rates. The parameters used to compute the performance metrics were those that maximized the posterior probability density, averaged across chains. Since the models were fit to R and M rates together, the Bayesian information criterion (BIC) and Gelman-Rubin index (G) are reported for both variables together, and were computed on the training datasets.

Variable	Performance index	Model 0	Model I	Model II	Model III
M and R	G	1.002	1.002	1.007	1.006
	BIC	−671.94	−830.72	−678.70	−832.05
R	R^2	0.71	0.92	0.70	0.91
M	R^2	0.23	0.36	0.26	0.36
R	RMSE (gC kg^{-1} d^{-1})	0.016	0.008	0.015	0.009
M	RMSE (gN kg^{-1} d^{-1})	0.002	0.001	0.001	0.001

Table 2
Equations of heterotrophic respiration and net N mineralization rates for the four model variants, with or without microbial biomass and diversity effects. The total number and list of calibrated parameters refer to models with constant k_0 and varying k_0 (in brackets). $k_{0,d}$, $k_{0,f}$, $k_{0,ow}$ denote the decay coefficients for dehesas, forests, and open woodlands, respectively.

Model	Equations	Microbial parameters	Total number of calibrated parameters	List of calibrated parameters
Model 0	$\begin{cases} R = (1-\mathrm{CUE})k_0 C_S \\ M = k_0 C_S\left[\frac{1}{(C:N)_S} - \frac{\mathrm{CUE}}{(C:N)_B}\right] \end{cases}$	$\gamma = 0;\ \beta = 0$	3 (5)	CUE, k_0, σ (CUE, $k_{0,d}$, $k_{0,f}$, $k_{0,ow}$, σ)
Model I	$\begin{cases} R = (1-\mathrm{CUE})k_0 C_S C_B^{\gamma} \\ M = k_0 C_S C_B^{\gamma}\left[\frac{1}{(C:N)_S} - \frac{\mathrm{CUE}}{(C:N)_B}\right] \end{cases}$	$\gamma \neq 0;\ \beta = 0$	4 (6)	CUE, k_0, σ, γ (CUE, $k_{0,d}$, $k_{0,f}$, $k_{0,ow}$, σ, γ)
Model II	$\begin{cases} R = (1-\mathrm{CUE})k_0 e^{\beta f_0} C_S \\ M = k_0 e^{\beta f_0} C_S\left[\frac{1}{(C:N)_S} - \frac{\mathrm{CUE}}{(C:N)_B}\right] \end{cases}$	$\gamma = 0;\ \beta \neq 0$	4 (6)	CUE, k_0, σ, β (CUE, $k_{0,d}$, $k_{0,f}$, $k_{0,ow}$, σ, β)
Model III	$\begin{cases} R = (1-\mathrm{CUE})k_0 e^{\beta f_0} C_S C_B^{\gamma} \\ M = k_0 e^{\beta f_0} C_S C_B^{\gamma}\left[\frac{1}{(C:N)_S} - \frac{\mathrm{CUE}}{(C:N)_B}\right] \end{cases}$	$\gamma \neq 0;\ \beta \neq 0$	5 (7)	CUE, k_0, σ, β, γ (CUE, $k_{0,d}$, $k_{0,f}$, $k_{0,ow}$, σ, β, γ)

Table 4
Results of the posterior parameter distributions obtained from Bayesian data assimilation with DRAM sampler. For each model (Table 2), the prior parameter ranges, as well as the mode (i.e., maximum a posteriori), the mean, and the 95 % confidence interval (CI) of the posterior parameter distributions, are shown (each metric was averaged across chains). The results for models II and III are based on the diversity index of combined fungal and bacterial richness ($f_0 = \sqrt{S_{fungi} S_{bacteria}}$) (Fig. 2.5). The results refer to models recalibrated on the entire dataset.

		Parameters				
		k_0	γ	β	CUE	σ
Model 0	Priors	$[10^{-6}; 1]$	–	–	$[10^{-6}; 1]$	$[10^{-6}; 1]$
	Mode	$7.4 \bullet 10^{-4}$	–	–	$3.2 \bullet 10^{-1}$	$1.2 \bullet 10^{-2}$
	Mean ± CI (95 %)	$7.9 \bullet 10^{-4} \pm 1.3 \bullet 10^{-5}$	–	–	$3.2 \bullet 10^{-1} \pm 1.0 \bullet 10^{-2}$	$1.2 \bullet 10^{-2} \pm 4.7 \bullet 10^{-5}$
Model I	Priors	$[10^{-6}; 1]$	$[10^{-6}; 1]$	–	$[10^{-6}; 1]$	$[10^{-6}; 1]$
	Mode	$2.4 \bullet 10^{-4}$	$9.0 \bullet 10^{-1}$	–	$3.4 \bullet 10^{-1}$	$5.6 \bullet 10^{-3}$
	Mean ± CI (95 %)	$2.4 \bullet 10^{-4} \pm 2.6 \bullet 10^{-6}$	$8.9 \bullet 10^{-1} \pm 3.1 \bullet 10^{-3}$	–	$3.2 \bullet 10^{-1} \pm 6.6 \bullet 10^{-3}$	$5.8 \bullet 10^{-3} \pm 2.3 \bullet 10^{-5}$
Model II	Priors	$[10^{-6}; 1]$	–	$[-0.1; 10^{-3}]$	$[10^{-6}; 1]$	$[10^{-6}; 1]$
	Mode	$2.1 \bullet 10^{-3}$	–	$-2.0 \bullet 10^{-3}$	$2.9 \bullet 10^{-1}$	$1.1 \bullet 10^{-2}$
	Mean ± CI (95 %)	$2.7 \bullet 10^{-3} \pm 7.6 \bullet 10^{-5}$	–	$-2.3 \bullet 10^{-3} \pm 4.0 \bullet 10^{-5}$	$3.2 \bullet 10^{-1} \pm 9.9 \bullet 10^{-3}$	$1.1 \bullet 10^{-2} \pm 4.4 \bullet 10^{-5}$
Model III	Priors	$[10^{-6}; 1]$	$[10^{-6}; 1]$	$[-0.1; 10^{-3}]$	$[10^{-6}; 1]$	$[10^{-6}; 1]$
	Mode	$4.0 \bullet 10^{-4}$	$8.9 \bullet 10^{-1}$	$-1.0 \bullet 10^{-3}$	$3.4 \bullet 10^{-1}$	$5.6 \bullet 10^{-3}$
	Mean ± CI (95 %)	$4.2 \bullet 10^{-4} \pm 8.2 \bullet 10^{-6}$	$8.9 \bullet 10^{-1} \pm 3.3 \bullet 10^{-3}$	$-1.0 \bullet 10^{-3} \pm 3.0 \bullet 10^{-5}$	$3.2 \bullet 10^{-1} \pm 6.7 \bullet 10^{-3}$	$5.7 \bullet 10^{-3} \pm 2.2 \bullet 10^{-5}$

using Markov Chain Monte Carlo (MCMC) simulations with an Adaptive Metropolis algorithm with Delayed-Rejection procedure (DRAM, Soetaert and Petzoldt, 2010) implemented in R (R Core Team, 2022). To assess the stationarity of the posterior probability distributions we ran three parallel MCMC chains and checked for convergence with the Gelman-Rubin diagnostic index (G). The threshold for G was set to 1.1 for all parameters, meaning that if G was lower than 1.1 the chains were considered to have converged to the stationary posteriors of the parameters (Brooks and Gelman, 1998).

In addition, we implemented a stratified calibration where k_0 was allowed to vary across the different land-uses (i.e., forests, woodlands, and dehesas). This approach aimed to assess the effects of litter quality and environmental conditions—both of which may differ across land-uses—on heterotrophic respiration and net N mineralization rates. Land-use-specific effects were thus assumed to modify the decomposition kinetics via the parameter k_0. For implementation requirements, this stratified calibration was developed relying on a Hamiltonian Monte Carlo with No-U-Turn Sampler (NUTS, Hoffman and Gelman (2014) implemented in STAN (Stan Development Team, 2024). Results comparing the constant and varying k_0 for the selected diversity index are shown in the Supplementary Material (Table S2). While NUTS is Hamiltonian and DRAM is based on a Metropolis-Hastings approach, both samplers are designed to respect the same assumptions and have been tested with the same likelihood function and convergence index (G).

2.9. Model validation

The different model variants (0, I, II, and III, with constant or varying k_0) were compared using the coefficient of determination (R^2), the root mean squared error (RMSE) and the Bayesian information criterion (BIC) for both heterotrophic respiration and net N mineralization rates. BIC allows comparing models regarding not only their performance, but also their parsimony, balancing goodness of fit and number of parameters (lower BIC values – even negative – indicate better balance). To check the validity of the results, we performed a 10-fold cross validation. This consists in splitting the data into 10 groups, and iteratively selecting one group for model evaluation while training the model on the rest (Fig. 2.4). Then, we averaged the performance indices of the models across all 10 iterations and reported them in Table 3 for comparison. For models including microbial diversity effects (i.e., models II and III), all results are reported for the diversity index based on the combined fungal and bacterial richness (Eq. (1)). This was done for convenience, since all diversity indices led to similar results (see Table S1 for the results with all diversity indices). Comparison of models with constant and varying k_0 for the selected diversity index of combined fungal and bacterial richness are also shown in the Supplementary Material (Table S2). The posterior distributions of the parameters were obtained by re-training the models on the whole dataset.

3. Results

3.1. Exploratory data analysis across land-uses

Microbial biomass was higher in forests and open woodlands, compared to dehesas (p-$value = 0.02$). Bacterial richness was higher in dehesas, compared to land-uses dominated by trees (p-$value = 0.02$), while fungal richness remained stable across land-uses (p-$value > 0.05$) (Fig. 3). Across all land-uses, heterotrophic respiration increased with increasing microbial biomass (Fig. 4a). This trend is indicative of an exponent $\gamma > 0$ in Eq. (3), suggesting that microbial biomass plays a significant role in SOC decomposition. Similarly, microbial biomass positively affected net N mineralization rates (Fig. 4b), although the proportion of variance explained by the linear regression was 4 times lower ($R^2 = 0.2$). This relationship also varied across land-uses, with dehesas exhibiting a steeper slope and open woodlands showing a greater variability (Fig. 4b and Fig. S2b). Average heterotrophic respiration slightly decreased with increasing microbial richness (Fig. 4c), while net N mineralization was not affected by microbial diversity (Fig. 4d). In both cases, the largest variability was found in open woodlands (Figs. S2c and S2d).

3.2. Performance of the models

Cross validation revealed that models incorporating microbial biomass yielded the best results, with models I and III outperforming models 0 and II in terms of R^2, RMSE, and BIC (Table 3). When compared to observations, model 0 showed similar results to model II for both heterotrophic respiration and net N mineralization rates (Table 3), indicating that microbial diversity effects were minor. Note that this was true for all diversity indices, including those that were calculated based on fungal functional groups (Table S1). Both models including biomass (i.e., models I and III) provided accurate predictions of heterotrophic respiration, with $R^2 > 0.9$ and minimal model bias despite having only four and five parameters, respectively (Fig. 5). In contrast, net N mineralization rate was predicted less well, with some overestimated values mostly corresponding to large measured net N mineralization rates (Fig. 5).

3.3. Microbial biomass effects

The posterior distributions of the estimated model parameters are

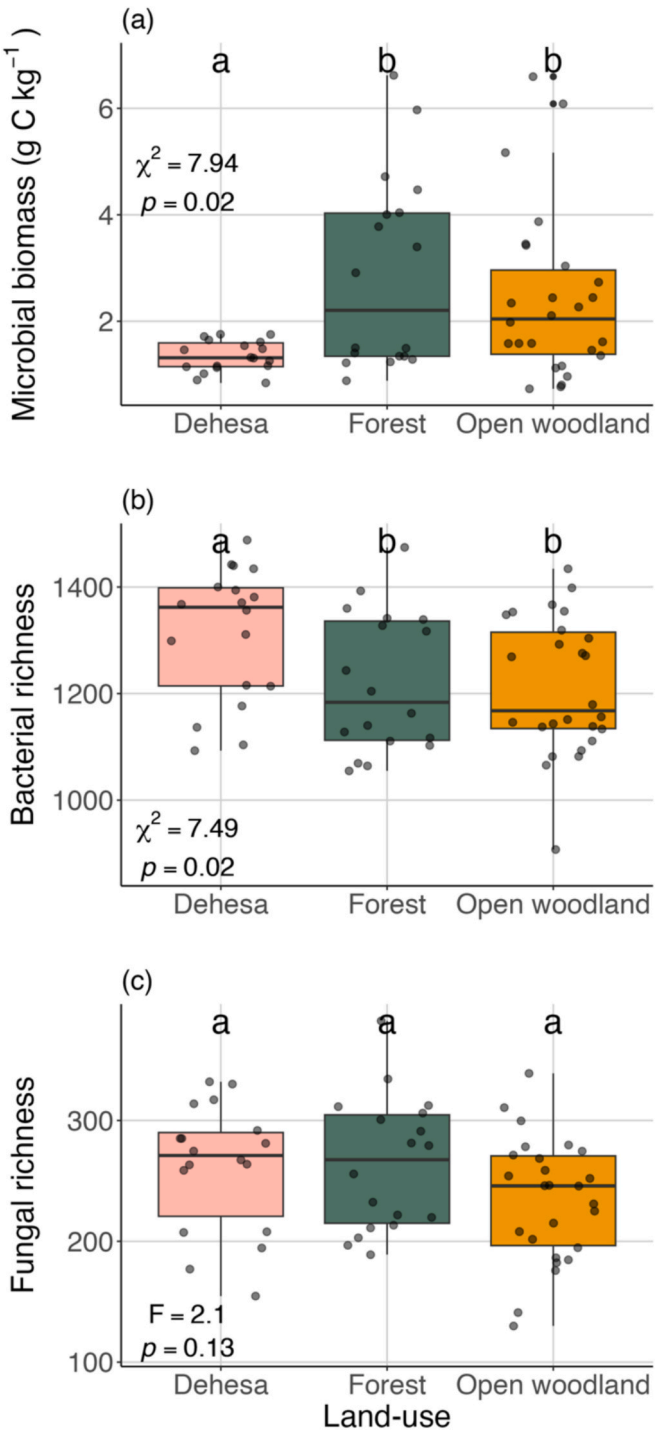

Fig. 3. Variations in (a) microbial biomass, (b) bacterial richness, and (c) fungal richness across the three land-uses: dehesas (n = 18), forests (n = 18), and open woodlands (n = 26). Median values for microbial biomass are 1.34, 2.87, and 2.41 (g C kg^{-1}), respectively; for bacterial richness, they are 1362, 1184, and 1168 (number of OTUs); and for fungal richness, they are 271, 268, and 246 (number of OTUs). Letters indicate whether data differ across land-uses, with the statistical test values and associated p-values indicated in the panels.

shown in Fig. 6. The results were consistent across the three MCMC chains (G < 1.01, Table 3) and across models (Fig. 6 and Table 4), suggesting that the estimated parameter values are reliable. As expected from the exploratory data analysis (Fig. 4), models I and III showed a significant and positive effect of the microbial biomass on the heterotrophic respiration (Table 4). In fact, the posterior probability distributions of the biomass exponent (γ) had a mean larger than zero (Table 4). In particular, the mean γ values were consistently close to 1 across models (Table 4), indicating an almost linear relationship between microbial biomass and heterotrophic respiration. In all models, CUE had a mean of about 0.3 (Table 4). However, in models that did not account for the effect of biomass, CUE had a much larger standard deviation (Fig. 6), suggesting that CUE values cannot be accurately estimated without microbial biomass.

3.4. Microbial diversity effects

The mean decay constants (k_0) are directly comparable between models 0 and II and between models I and III since they have nearly identical biomass exponents (γ). The mean values of the decay constant were lower in models 0 and I, which only considered microbial biomass, compared to models II and III, respectively, which also accounted for microbial diversity. This suggests that incorporating diversity affects the decay rate constant. In particular, microbial diversity had a negative effect on heterotrophic respiration and net N mineralization. The diversity exponent β had a unimodal distribution with the best value (i.e., mode) of $-2 \bullet 10^{-3}$ and $-1 \bullet 10^{-3}$ in models II and III, respectively, indicating a small but negative effect of diversity on heterotrophic respiration and net N mineralization rates (Table 4). Nevertheless, this effect is small, and retaining the diversity rate modifier from Eq. (6) increases model complexity without substantial gains in model performance.

4. Discussion

4.1. Microbial biomass effects on heterotrophic respiration and net N mineralization

4.1.1. Microbial biomass drives heterotrophic respiration

Our results suggest that heterotrophic respiration is mainly controlled by both SOC substrate quantity and microbial biomass. In particular, data assimilation indicated a positive and nearly linear relationship between microbial biomass and heterotrophic respiration ($\gamma \approx 1$; Fig. 4a). This result aligns with previous studies that show a significant association between microbial biomass and heterotrophic respiration rate (Colman and Schimel, 2013; Hartman and Richardson, 2013). Notably, most soil C and N cycling models assume linear kinetics with respect to SOC ($\gamma = 0$) (Manzoni and Porporato, 2009; Le Noë et al., 2023), meaning that respiration is driven only by the amount of available C substrates. In contrast, here we demonstrate that respiration kinetics vary as a function of microbial biomass and can be well represented by a multiplicative function of SOC and microbial biomass C (a model previously considered for its simplicity; e.g., Manzoni and Porporato, 2007). The respiration kinetics in Eq. (3) can also be rearranged to calculate the microbial metabolic quotient (i.e., respiration rate over microbial biomass C, $R/C_B = k_R C_S C_B^{\gamma-1}$), which in our multiplicative model varies linearly with SOC (i.e., $R/C_B \approx k_R C_S$, as $\gamma \approx 1$). On a global scale, structural equation modeling has shown that SOC is both negatively (directly) and positively (indirectly) associated with the microbial metabolic quotient. The direct negative association likely reflects higher substrate quality in SOC-rich soils, which enhances microbial efficiency in allocating C to growth and leads to a lower R/C_B. In contrast, the indirect positive association, mediated by microbial basal respiration, was found to be stronger than the negative direct effect (Xu et al., 2017). This means that although higher SOC directly reduces respiration per unit of microbial biomass, it also stimulates microbial activity, which in turn raises respiration rates. Considering both pathways, the net result is that higher SOC levels tend to increase the heterotrophic respiration rate per unit of microbial biomass, primarily through SOC indirect effect on microbial respiration. These findings

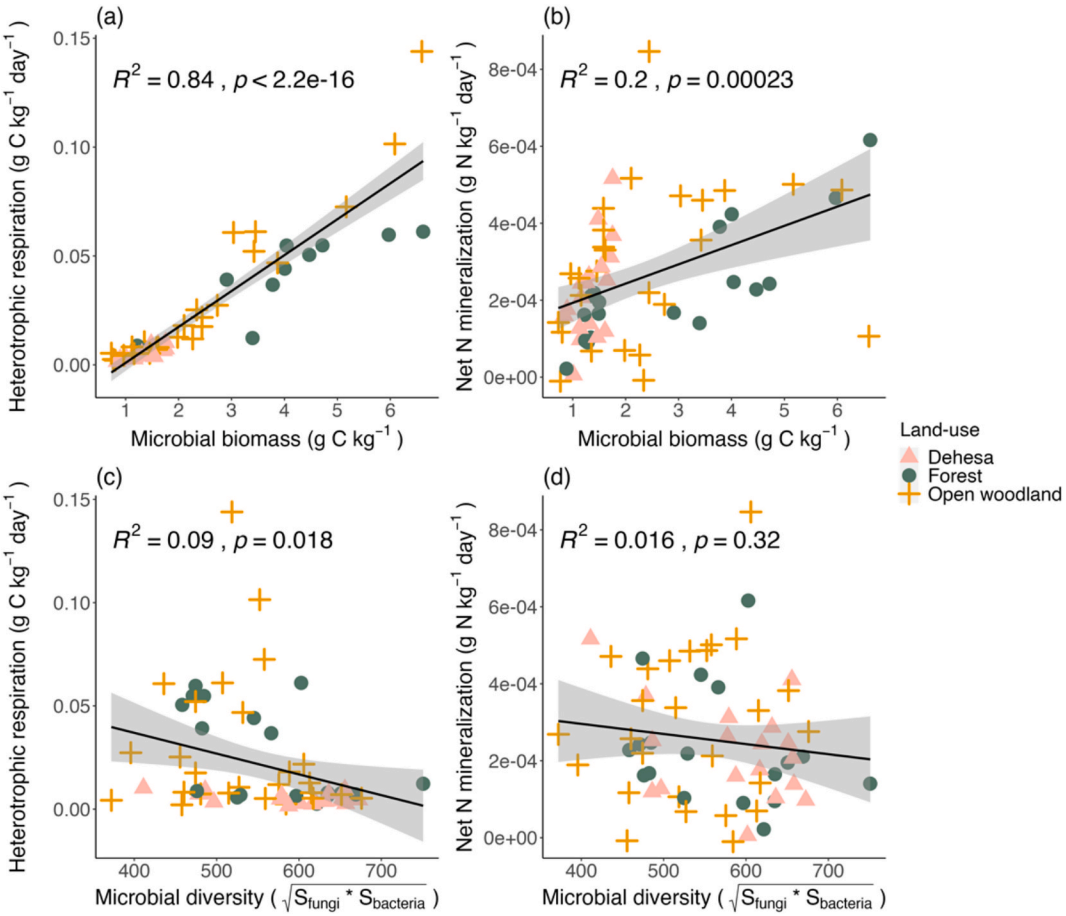

Fig. 4. Relationships in observations between (a) heterotrophic respiration and microbial biomass, (b) net N mineralization and microbial biomass, (c) heterotrophic respiration and microbial diversity (combined fungal and bacterial richness), and (d) net N mineralization and microbial diversity (combined fungal and bacterial richness). Points from different land-uses (dehesa, forest, open woodland) are highlighted with different colors and shapes. For each linear regression, R^2 denotes the coefficient of determination, and p-values reflect the significance of the regression coefficients (n = 62).

suggest that microbial activity and biomass jointly mediate the effects of SOC on C fluxes, and highlights the need to explicitly represent microbial biomass in ecosystem models to better capture SOC-respiration dynamics. It is therefore crucial to accurately constrain microbial biomass dynamics through direct assimilation of observations in order to effectively represent C and N mineralization rates in ecosystem models.

4.1.2. Coupled C and N cycles

The net N mineralization rates follow the patterns found for respiration rates as in Setälä and McLean (2004), highlighting the tight coupling between the C and N cycles (Manzoni et al., 2010; Guenet et al., 2021). This link can be explained by microbial metabolism—higher rates of C uptake and respiration are associated with higher rates of N uptake (e.g., $R^2 \approx 0.45$ between C and N uptake rates estimated from data in Colman and Schimel (2013)). When N acquired from organic matter exceeds microbial stoichiometric requirements, it is released in mineral form (Ågren and Bosatta, 1998). This process typically occurs in mineral soils where the C:N ratio is below the threshold element ratio, indicating conditions of C limitation and N excess. In our data, the majority of sites had organic matter C:N ratios lower than the estimated average threshold element ratio, $\mathrm{TER} = (C:N)_B / CUE \approx 22$ (considering $(C:N)_B = 7$ (Xu et al., 2013) and $CUE \approx 0.32$ from model fitting). As a result of generally sufficient N availability, the net N mineralization rate in C-limited soils is proportional to the rates of C uptake and respiration. Therefore, the positive effect of microbial biomass on heterotrophic respiration propagates further to the N cycle, resulting in the positive correlation between microbial biomass and the net N mineralization rate observed at the regional scale in this study (Fig. 4b) and at the global scale in the work of Li et al. (2019). Among the three sites with a substrate C:N ratio higher than the estimated average TER (i.e., Almería, Alicante, and León), only Almería actually exhibited net N immobilization in the measurements. However, our TER estimate is based on average $(C:N)_B$ values from mixed and temperate forests reported by Xu et al. (2013), which may not correspond to actual on-site values. Similarly, CUE likely varies between sites due to differences in substrate quality or environmental conditions – factors we only partially accounted for through Bayesian data assimilation by assigning a probability distribution to the CUE parameter. It is thus possible that at certain sites N was more limiting than we would expect from the average TER.

4.1.3. Differences across land-use

Similar to Li et al. (2019), Figs. 4b and S2b also reveal a strong interaction between land-use and microbial biomass in explaining net N mineralization. Indeed, in dehesas and forests, the net N mineralization rate is positively correlated with microbial biomass, although in dehesas this relationship is much steeper (Fig. S2b). In contrast, open woodlands exhibit a larger variability in the relationship between microbial biomass and net N mineralization. This may be partly due to their habitat heterogeneity (e.g., floristic composition and tree density) and broader geographical distribution (Fig. 1), suggesting effects of both biotic (e.g., litter quality) and abiotic factors (e.g., different exposure to solar radiation and other microclimatic conditions) on net N

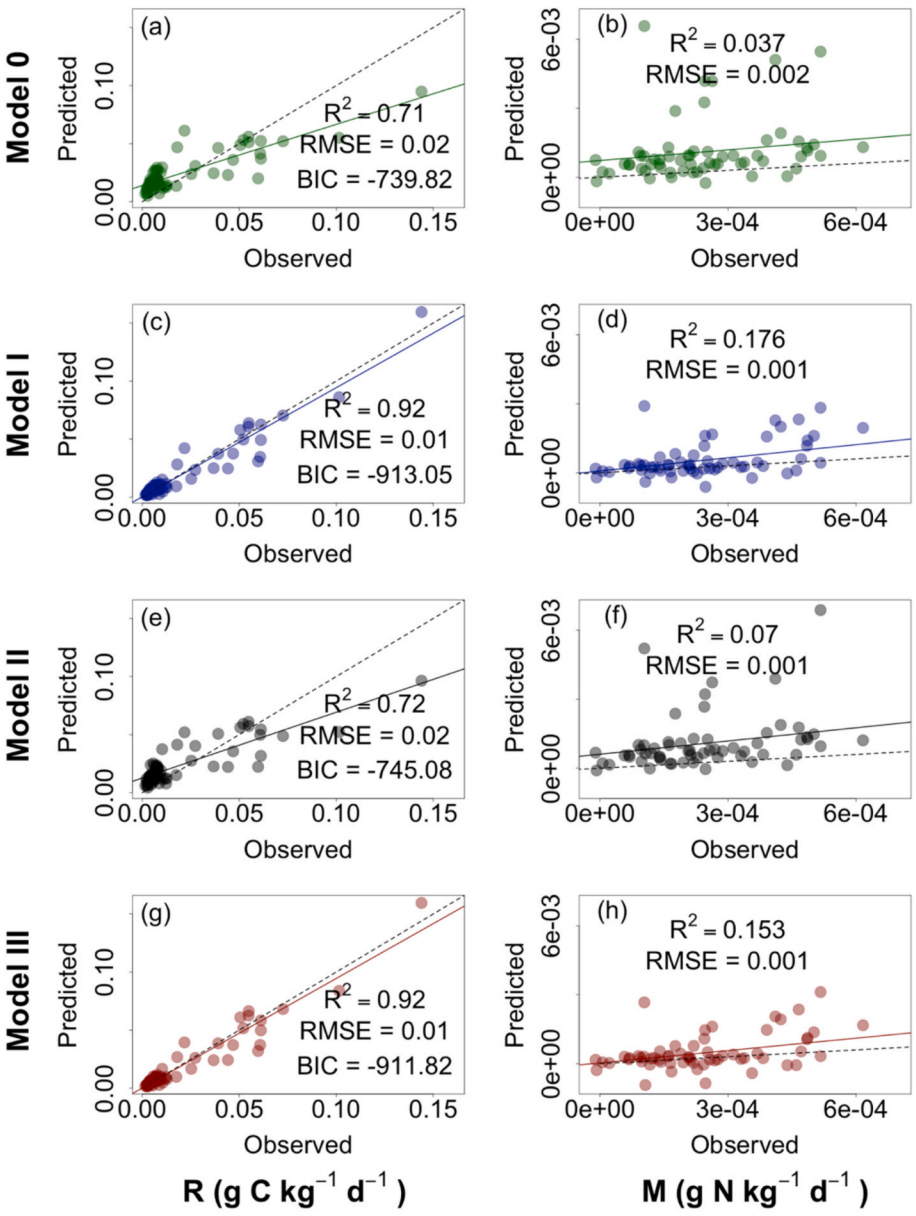

Fig. 5. Predicted versus observed heterotrophic respiration (R) and net N mineralization rates (M) for models 0, I, II, and III (with $f_0 = \sqrt{S_{fungi} S_{bacteria}}$) (Table 3). The parameters used for model predictions were those that maximized the posterior probability density functions, averaged across chains. The dashed black line indicates the 1:1 relationship, while the colored lines represent the linear regressions between predicted and observed values. Note that performance indices (R^2, RMSE, and BIC) refer to the performance of the models trained on the whole dataset.

mineralization rates (Li et al., 2019).

In the models, this land-use effect is reflected in the stratified calibration results of the decay rate constant (k_0), which affects both the heterotrophic respiration and the net N mineralization. The results indicated a lower decay rate constant (k_0) in dehesas compared to the other land-uses (Fig. S4). Differences across land-uses are likely driven by differences in organic inputs, nutrients' stoichiometry, and altered soil physico-chemical properties. García-Angulo et al. (2020) and Gazol et al. (2021) showed that, across these land-uses, dehesas had the lowest crown coverage and pH, and these conditions were associated with a higher abundance of nitrifying bacteria. Due to the presence of grazing, dehesas tend to be richer in N (García-Angulo et al., 2020), and here we also showed that they had lower microbial biomass relative to forests and open woodlands (Fig. 3a). This suggests that ecosystems with low C: N ratios can sustain high net N mineralization despite having low microbial biomass (Figs. 4b andS2b).

4.2. *Microbial diversity effects on heterotrophic respiration and net N mineralization rates*

Contrary to our expectation that microbial diversity would promote heterotrophic respiration and net N mineralization rates, we found that diversity had only minor and negative effects on these processes (Table 4, Fig. S3). It is possible that in soils with already highly diverse, and possibly redundant, microbial communities, variations in bacterial and fungal diversity across land-uses are not sufficiently large to have predictive power (Setälä and McLean, 2004; Wohl et al., 2004). Instead, in low-diversity communities (e.g., manipulated under laboratory conditions), increasing diversity promotes both decomposition and respiration (Setälä and McLean, 2004; Bell et al., 2005; Tiunov and Scheu, 2005; Wilkinson et al., 2012; Valentin et al., 2014; Domeignoz-Horta et al., 2020). In fact, some function-diversity relationships are hump-shaped, with a positive diversity effect as long as diversity is low, then

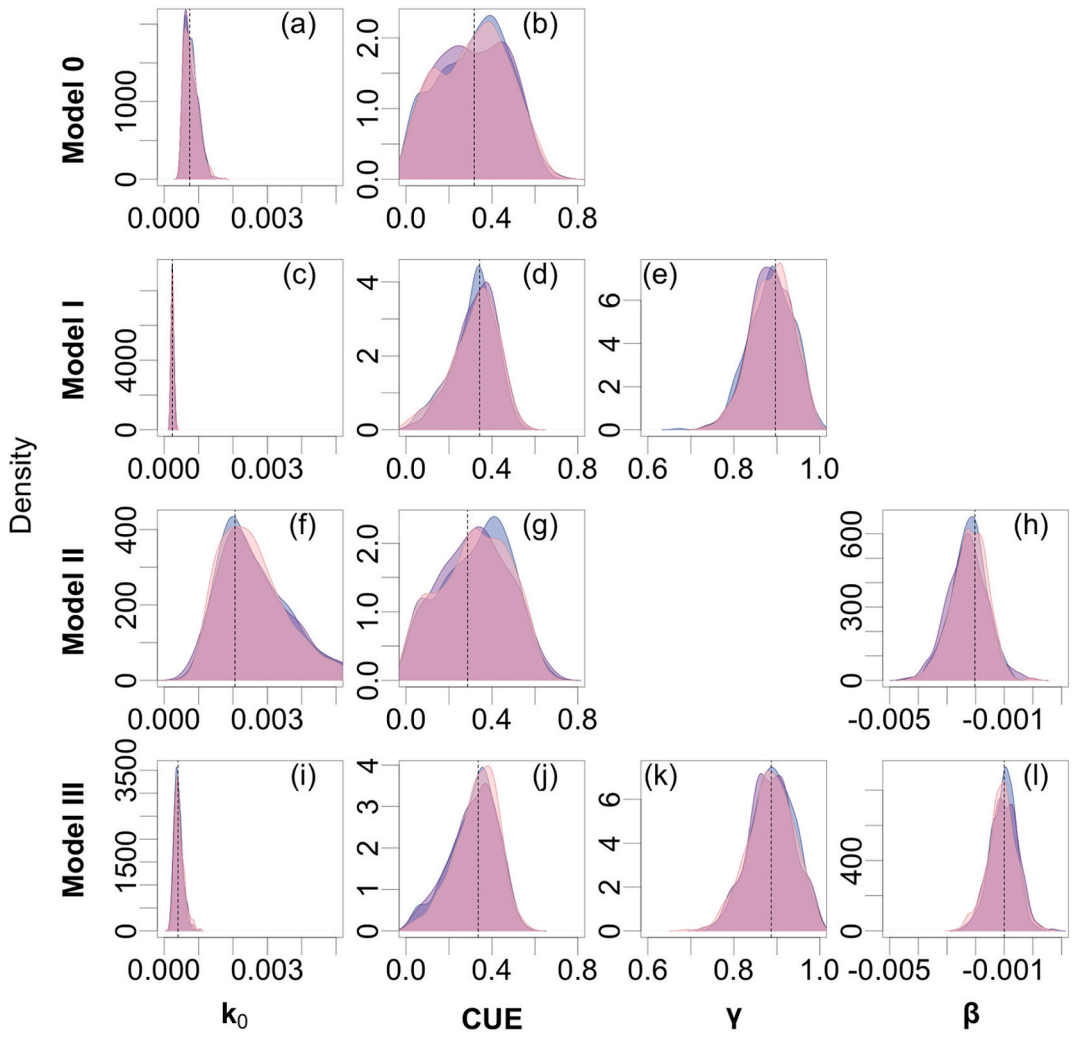

Fig. 6. Posterior probability density functions of the parameters for (a–b) model 0, (c–e) model I, (f–h) model II, and (i–l) model III for the three MCMC chains. The dashed vertical lines indicate the modes of the parameters (i.e., the maximum a posteriori), averaged across chains. The results for models II and III are based on the combined fungal and bacterial richness ($f_0 = \sqrt{S_{fungi} S_{bacteria}}$). The posterior distributions were obtained from models retrained on the entire dataset.

turning to a negative effect as competitive interactions begin to dominate at high diversity levels (Nielsen et al., 2011; Pennekamp et al., 2018). This pattern would be consistent with the positive diversity effect found in laboratory studies with manipulated communities, and the slightly negative effects in the dataset analyzed here. For example, interspecific interactions in fungal communities can reduce community-level CUE (Maynard et al., 2017)—an indication of altered metabolism in the presence of competitors. The data analyzed here does not allow quantifying diversity effects resulting from the loss of large fractions of the community after disturbance or forest management, which were not part of the sampling design in García-Angulo et al. (2020). Our results are also not consistent with the global relationships found between microbial diversity and soil multifunctionality (Delgado-Baquerizo et al., 2017). However, the definition of multifunctionality includes a set of variables that do not necessarily reflect the functioning of microbial communities, such as the concentrations of specific nutrients or the amount of DNA, which are likely to covary with SOC. In contrast, our study covers a broad range of soils and is designed to test the specific effect of microbial diversity on key functions of the heterotrophic community related to both C and N cycling.

4.3. Limitations and uncertainties of this study

García-Angulo et al. (2020) showed that tree health significantly contributed to explaining variations in mineralization rates, with healthier trees increasing heterotrophic respiration while reducing net N mineralization. This underscores a potential limitation of the C-N model presented here, as changes in microbial community composition within the same site were treated as intra-site variability and not directly linked to tree health conditions, which may influence microbial activity and the C-N cycles. However, adding this level of complexity would have increased the number of parameters to calibrate, possibly leading to identifiability issues and larger uncertainties in the models. Instead, the effect of tree health status was indirectly accounted for via the soil variables explicitly included in the model (i.e., soil organic C, C:N ratio, microbial biomass, and microbial diversity).

In our modeling framework, model 0 suffered from parameter identifiability issues, with parameters *CUE* and k_0 being highly and positively correlated (r = 0.95, Fig. S5). In general, k_0 was positively correlated to *CUE* and negatively correlated to γ and β (Fig. S5). Adding microbial biomass to the models reduced identifiability issues, as the parameters had unimodal posterior distributions with lower standard deviations compared to models without biomass (Fig. 6). This result further emphasizes that adding microbial biomass strengthened model reliability while also improving the interpretability of the biological processes represented.

Overall, it is crucial to carefully balance model complexity and performance to ensure robust and reliable predictions (Luo et al., 2009;

Shi et al., 2018). Adding biological variables to a soil C and N cycling model is now considered as a necessary step towards more accurate predictions, but this increased complexity should be matched by an increased number of measured variables to constrain the new model parameters (Saifuddin et al., 2021; Manzoni and Schimel, 2024). Microbial biomass measurements offer opportunities to reach this goal, while here we show that including diversity metrics does not allow increasing performance or robustness.

4.4. Linking microbial diversity to ecosystem functions

4.4.1. Taxonomic vs. functional diversity

Given the extreme complexity of microbial communities, it is not feasible to include all their characteristics in ecosystem models. Therefore, establishing an optimal level of model complexity is essential for integrating microbial diversity, but how to reach this goal remains an open question (Lennon et al., 2024). Our study highlights the knowledge gap in understanding the relationship between microbial diversity and ecosystem functions when diversity metrics are based on taxonomic identification. While taxonomic metrics are the state-of-the-art approach for studying biodiversity effects on ecosystem functions (Bahram et al., 2018; Delgado-Baquerizo et al., 2018), they were in many cases developed for studying other kingdoms (i.e., plants and animals), and may be inappropriate measures of the functional diversity for microbial communities (Crowther et al., 2019). This limitation arises from factors such as functional redundancy, dormancy, and phenotypic plasticity, in addition to the spatial and temporal heterogeneity of microbial characteristics (Hall et al., 2018; Malik et al., 2020). This is particularly true for prokaryotes, for which associating specific functions is challenging due to their high replication rates, horizontal gene transfer (HGT), and extensive diversity. As a result, bacteria affiliated with, for instance, a methylo-genus do not necessarily exhibit methanotrophic activity, which is why genome assembly is often necessary to infer functions accurately. In contrast, functional associations for fungi tend to be more predictable; for instance, saprotrophic fungi are the primary decomposers of OM in forests, while ectomycorrhizal fungi form symbiotic relationships with trees, exchanging N and phosphorus for sugars (Crowther et al., 2019). In our study, we tested broad functional groups based on taxonomic identification (i.e., bacteria, fungi, and saprotrophic and ectomycorrhizal fungi), which represent distinct ecological roles and were expected to serve as proxies for the influence of functional diversity on mineralization rates. However, our results showed that, independently of the microbial group considered, diversity had only a small and negative effect on C and N mineralization rates.

4.4.2. Microbial functional traits and ecosystem functions

To understand their functional capabilities, microbial taxa could be grouped based on physiological or eco-physiological traits, for instance, their metabolic strategies, resource acquisition mechanisms, carbon use efficiency, or greenhouse gas production capacity – which are directly linked to ecosystem functions. Focusing on microbial functional traits is a promising way to bridge this gap and could provide deeper insights into how microbial communities drive ecosystem functions (Allison et al., 2010; Crowther et al., 2014). Despite its potential, research on microbial functional traits remains underdeveloped. There is a pressing need to quantify how shifts in microbial traits affect key ecosystem processes like nutrient cycling, OM decomposition, and C sequestration, and to identify how phenotypic traits can be efficiently synthesized into functional groups. Microbial functional groups can synthesize community composition and reflect its effect on ecosystem functions. For example, the copiotroph – oligotroph continuum (Koch, 2001; Fierer et al., 2007), which has also been applied to the microbial explicit ecosystem model MIMICS (Wieder et al., 2015), or classifications based on life history strategies, i.e., the growth yield, resource acquisition, and stress tolerance tradeoff framework (Y-A-S) (Malik et al., 2020), could offer avenues for capturing key axes of variation in the microbial communities. Databases like FungalTraits already provide guild classifications that can be associated to ecological traits (Põlme et al., 2021). Omics approaches such as metagenomics and metatranscriptomics (for gene presence and gene expression, respectively) provide complementary insights for linking community-level microbial traits to ecosystem functions. Recently, Li et al. (2025) showed that integrating genome-inferred microbial traits into an ecosystem model improved the predictions of methane emissions in a permafrost site. Incorporating phylogenetic indices that account for evolutionary relationships among species could also strengthen the signal of diversity on ecosystem functioning, as certain microbial traits are phylogenetically conserved (Martiny et al., 2015). By reflecting shared evolutionary history and functional similarities, phylogenetic indices may help predict trait functions across species and their effects on ecosystem processes. Recent frameworks have also emphasized the importance of examining compositional shifts in microbial communities over different timescales and understanding the mechanisms by which these changes influence community functions (Abs et al., 2024). This is particularly relevant, as interspecific interactions—such as competition—may have influenced the observed mineralization rates in these ecosystems, pointing to mechanisms beyond simple diversity effects.

4.4.3. Future research directions

In general, efforts should be directed toward acquiring new genomes to better understand the ecological attributes of dominant soil microbial taxa (Delgado-Baquerizo et al., 2018). Then, understanding which taxa are related to specific microbial traits and assessing their relative abundance, will help us gain insights into the effects of diversity on ecosystem functioning and C cycling. In addition, omics strategies can help to link microbial traits to ecosystem processes. As omics data becomes increasingly available, future research should focus on applying these approaches to unlock the connections between microbial community composition and ecosystem dynamics. Developing meaningful measures of microbial diversity for heterogenous soil systems such as those used in this study may also require aligning these metrics with the spatial and temporal scales at which microbial processes occur (Dini-Andreote et al., 2021). Ultimately, at larger scales, microbial community composition and traits may be largely responsive to changes in resource availability and abiotic conditions, potentially reducing the need to explicitly incorporate microbial diversity into models. In our study, microbial diversity did not emerge as a primary driver of heterotrophic respiration and net N mineralization, but it may still be critical under different ecological conditions or in regulating other ecosystem processes. The influence of microbial functions on ecosystem processes still requires further investigation to determine if and which microbial traits should be integrated into ecosystem models.

5. Conclusions

We applied a simple model of soil C and N dynamics to evaluate the effects of microbial biomass and diversity on heterotrophic respiration and net N mineralization rates. Our findings show that microbial biomass had a strong and positive effect on both heterotrophic respiration and net N mineralization rates, with heterotrophic respiration being nearly linearly correlated with microbial biomass. In contrast, integrating microbial diversity as a rate modifier exerted only slight and negative effects on these processes. Notably, heterotrophic respiration and net N mineralization rates were modeled equally well by equations with and without microbial diversity. Hence, adding a parameter to describe diversity effects is not justifiable according to the Bayesian information criterion. We conclude that microbial biomass plays a crucial role in controlling C dynamics and should be incorporated into ecosystem models, while further research is needed to determine whether and how microbial diversity should be integrated.

CRediT authorship contribution statement

Elisa Bruni: Writing – original draft, Methodology, Formal analysis, Conceptualization. **Jorge Curiel Yuste:** Writing – review & editing, Data curation, Conceptualization. **Lorenzo Menichetti:** Writing – review & editing, Formal analysis. **Omar Flores:** Writing – review & editing, Data curation. **Daniela Guasconi:** Writing – review & editing, Formal analysis. **Bertrand Guenet:** Writing – review & editing, Supervision, Conceptualization. **Ana-Maria Hereș:** Writing – review & editing, Data curation. **Aleksi Lehtonen:** Writing – review & editing, Project administration, Funding acquisition. **Raisa Mäkipää:** Writing – review & editing, Project administration, Funding acquisition. **Marleen Pallandt:** Writing – review & editing. **Leticia Pérez-Izquierdo:** Writing – review & editing, Formal analysis. **Etienne Richy:** Writing – review & editing. **Mathieu Santonja:** Writing – review & editing. **Boris Tupek:** Writing – review & editing. **Stefano Manzoni:** Writing – original draft, Supervision, Methodology, Conceptualization.

Declaration of competing interest

The authors declare that they have no known competing financial interests or personal relationships that could have appeared to influence the work reported in this paper.

Acknowledgements

We acknowledge the work by Daniel García-Angulo for conducting the soil sampling and bio-chemical analysis that informed this study.

Funding

This work was funded by the grant "Holistic management practices, modelling and monitoring for European forest soils"—HoliSoils (H2020 grant agreement 101000289).

Appendix A. Supplementary data

Supplementary data to this article can be found online at https://doi.org/10.1016/j.geoderma.2025.117408.

Data availability

Datasets analyzed are available at: www.ncbi.nlm.nih.gov/sra, under BioProject accession no PRJNA529407. Codes are accessible at: https://github.com/elisabruni/CNmodel_diversity.

References

Abramoff, R., Xu, X., Hartman, M., O'Brien, S., Feng, W., Davidson, E., Finzi, A., Moorhead, D., Schimel, J., Torn, M., Mayes, M.A., 2018. The Millennial model: in search of measurable pools and transformations for modeling soil carbon in the new century. Biogeochemistry 137, 51–71. https://doi.org/10.1007/s10533-017-0409-7.

Abramoff, R.Z., Davidson, E.A., Finzi, A.C., 2017. A parsimonious modular approach to building a mechanistic belowground carbon and nitrogen model. J. Geophys. Res. Biogeo. 122, 2418–2434. https://doi.org/10.1002/2017JG003796.

Abs, E., Chase, A.B., Manzoni, S., Ciais, P., Allison, S.D., 2024. Microbial evolution—An under-appreciated driver of soil carbon cycling. Glob. Chang. Biol. 30, e17268. https://doi.org/10.1111/gcb.17268.

Ågren, G.I., Bosatta, E., 1998. Theoretical ecosystem ecology. Understanding element cycles. Cambridge University Press, Cambridge, United Kingdom.

Allison, S.D., Wallenstein, M.D., Bradford, M.A., 2010. Soil-carbon response to warming dependent on microbial physiology. Nat. Geosci. 3, 336–340. https://doi.org/10.1038/ngeo846.

Anderson, J.P.E., Domsch, K.H., 1978. A physiological method for the quantitative measurement of microbial biomass in soils. Soil Biol. Biochem. 10, 215–221. https://doi.org/10.1016/0038-0717(78)90099-8.

Bahram, M., Hildebrand, F., Forslund, S.K., Anderson, J.L., Soudzilovskaia, N.A., Bodegom, P.M., Bengtsson-Palme, J., Anslan, S., Coelho, L.P., Harend, H., Huerta-Cepas, J., Medema, M.H., Maltz, M.R., Mundra, S., Olsson, P.A., Pent, M., Põlme, S., Sunagawa, S., Ryberg, M., Tedersoo, L., Bork, P., 2018. Structure and function of the global topsoil microbiome. Nature 560, 233–237. https://doi.org/10.1038/s41586-018-0386-6.

Bastida, F., Eldridge, D.J., García, C., Kenny Png, G., Bardgett, R.D., Delgado-Baquerizo, M., 2021. Soil microbial diversity–biomass relationships are driven by soil carbon content across global biomes. ISME J. 15, 2081–2091. https://doi.org/10.1038/s41396-021-00906-0.

Bell, T., Newman, J.A., Silverman, B.W., Turner, S.L., Lilley, A.K., 2005. The contribution of species richness and composition to bacterial services. Nature 436, 1157–1160. https://doi.org/10.1038/nature03891.

Berardi, D.M., Hartman, M.D., Brzostek, E.R., Bernacchi, C.J., DeLucia, E.H., von Haden, A.C., Kantola, I., Moore, C.E., Yang, W.H., Hudiburg, T.W., Parton, W.J., 2024. Microbial-explicit processes and refined perennial plant traits improve modeled ecosystem carbon dynamics. Geoderma 443 (2024), 116851.

Berg, B., McClaugherty, C.A., 2020. Plant Litter. Decomposition, Humus Formation, Carbon Sequestration, 4th ed. Springer, Cham.

Beule, L., Karlovsky, P., 2020. Improved normalization of species count data in ecology by scaling with ranked subsampling (SRS): application to microbial communities. PeerJ 8, e9593. https://doi.org/10.7717/peerj.9593.

Bever, J.D., Platt, T.G., Morton, E.R., 2012. Microbial population and community dynamics on plant roots and their feedbacks on plant communities. Annu. Rev. Microbiol. 66, 265–283. https://doi.org/10.1146/annurev-micro-092611-150107.

Birch, H.F., 1958. The effect of soil drying on humus decomposition and nitrogen availability. Plant Soil 10, 9–31.

Bird, J.A., Kleber, M., Torn, M.S., 2008. 13C and 15N stabilization dynamics in soil organic matter fractions during needle and fine root decomposition. Org. Geochem.

Blagodatskaya, E., Kuzyakov, Y., 2013. Active microorganisms in soil: critical review of estimation criteria and approaches. Soil Biol. Biochem. 67, 192–211. https://doi.org/10.1016/j.soilbio.2013.08.024.

Brooks, S.P., Gelman, A., 1998. General methods for monitoring convergence of iterative simulations. J. Comput. Graph. Stat. 7, 434–455. https://doi.org/10.1080/10618600.1998.10474787.

Bruni, E., Chenu, C., Abramoff, R.Z., Baldoni, G., Barkusky, D., Clivot, H., Huang, Y., Kätterer, T., Pikuła, D., Spiegel, H., Virto, I., Guenet, B., 2022. Multi-modelling predictions show high uncertainty of required carbon input changes to reach a 4‰ target. Eur. J. Soil Sci. 73, e13330. https://doi.org/10.1111/ejss.13330.

Caporaso, J.G., Kuczynski, J., Stombaugh, J., Bittinger, K., Bushman, F.D., Costello, E.K., Fierer, N., Peña, A.G., Goodrich, J.K., Gordon, J.I., Huttley, G.A., Kelley, S.T., Knights, D., Koenig, J.E., Ley, R.E., Lozupone, C.A., McDonald, D., Muegge, B.D., Pirrung, M., Reeder, J., Sevinsky, J.R., Turnbaugh, P.J., Walters, W.A., Widmann, J., Yatsunenko, T., Zaneveld, J., Knight, R., 2010. QIIME allows analysis of high-throughput community sequencing data. Nat. Methods 7, 335–336. https://doi.org/10.1038/nmeth.f.303.

Cavicchioli, R., Ripple, W.J., Timmis, K.N., Azam, F., Bakken, L.R., Baylis, M., Behrenfeld, M.J., Boetius, A., Boyd, P.W., Classen, A.T., Crowther, T.W., Danovaro, R., Foreman, C.M., Huisman, J., Hutchins, D.A., Jansson, J.K., Karl, D.M., Koskella, B., Mark Welch, D.B., Martiny, J.B.H., Moran, M.A., Orphan, V.J., Reay, D. S., Remais, J.V., Rich, V.I., Singh, B.K., Stein, L.Y., Stewart, F.J., Sullivan, M.B., Van Oppen, M.J.H., Weaver, S.C., Webb, E.A., Webster, N.S., 2019. Scientists' warning to humanity: microorganisms and climate change. Nat. Rev. Microbiol. 17, 569–586. https://doi.org/10.1038/s41579-019-0222-5.

Cheng, W., Virginia, R.A., 1993. Measurement of microbial biomass in arctic tundra soils using fumigation-extraction and substrate-induced respiration procedures. Soil Biol. Biochem. 25, 135–141. https://doi.org/10.1016/0038-0717(93)90251-6.

Cole, J.R., Wang, Q., Fish, J.A., Chai, B., McGarrell, D.M., Sun, Y., Brown, C.T., Porras-Alfaro, A., Kuske, C.R., Tiedje, J.M., 2014. Ribosomal Database Project: data and tools for high throughput rRNA analysis. Nucleic Acids Res. 42, D633–D642. https://doi.org/10.1093/nar/gkt1244.

Coleman, K., Jenkinson, D.S., 1996. RothC-26.3 - a Model for the turnover of carbon in soil. In: Powlson, D.S., Smith, P., Smith, J.U. (Eds.), Evaluation of Soil Organic Matter Models. Springer, Berlin Heidelberg, Berlin, Heidelberg, pp. 237–246 doi: 10.1007/978-3-642-61094-3_17.

Colman, B.P., Schimel, J.P., 2013. Drivers of microbial respiration and net N mineralization at the continental scale. Soil Biol. Biochem. 60, 65–76. https://doi.org/10.1016/j.soilbio.2013.01.003.

Cotrufo, M.F., Wallenstein, M.D., Boot, C.M., Denef, K., Paul, E., 2013. The Microbial Efficiency-Matrix Stabilization (MEMS) framework integrates plant litter decomposition with soil organic matter stabilization: do labile plant inputs form stable soil organic matter? Glob. Chang. Biol. 19, 988–995. https://doi.org/10.1111/gcb.12113.

Crowther, T.W., Maynard, D.S., Crowther, T.R., Peccia, J., Smith, J.R., Bradford, M.A., 2014. Untangling the fungal niche: the trait-based approach. Front. Microbiol. 5. https://doi.org/10.3389/fmicb.2014.00579.

Crowther, T.W., van den Hoogen, J., Wan, J., Mayes, M.A., Keiser, A.D., Mo, L., Averill, C., Maynard, D.S., 2019. The global soil community and its influence on biogeochemistry. Science 365, eaav0550. https://doi.org/10.1126/science.aav0550.

Delgado-Baquerizo, M., Maestre, F.T., Reich, P.B., Jeffries, T.C., Gaitan, J.J., Encinar, D., Berdugo, M., Campbell, C.D., Singh, B.K., 2016. Microbial diversity drives multifunctionality in terrestrial ecosystems. Nat. Commun. 7, 10541. https://doi.org/10.1038/ncomms10541.

Delgado-Baquerizo, M., Oliverio, A.M., Brewer, T.E., Benavent-González, A., Eldridge, D. J., Bardgett, R.D., Maestre, F.T., Singh, B.K., Fierer, N., 2018. A global atlas of the dominant bacteria found in soil. Science 359, 320–325. https://doi.org/10.1126/science.aap9516.

Delgado-Baquerizo, M., Trivedi, P., Trivedi, C., Eldridge, D.J., Reich, P.B., Jeffries, T.C., Singh, B.K., 2017. Microbial richness and composition independently drive soil

multifunctionality. Funct. Ecol. 31, 2330–2343. https://doi.org/10.1111/1365-2435.12924.
Dini-Andreote, F., Kowalchuk, G.A., Prosser, J.I., Raaijmakers, J.M., 2021. Towards meaningful scales in ecosystem microbiome research. Environ. Microbiol. 23, 1–4. https://doi.org/10.1111/1462-2920.15276.
Domeignoz-Horta, L.A., Cappelli, S.L., Shrestha, R., Gerin, S., Lohila, A.K., Heinonsalo, J., Nelson, D.B., Kahmen, A., Duan, P., Sebag, D., Verrecchia, E., Laine, A.-L., 2024. Plant diversity drives positive microbial associations in the rhizosphere enhancing carbon use efficiency in agricultural soils. Nat. Commun. 15, 8065. https://doi.org/10.1038/s41467-024-52449-5.
Domeignoz-Horta, L.A., Pold, G., Liu, X.-J.-A., Frey, S.D., Melillo, J.M., DeAngelis, K.M., 2020. Microbial diversity drives carbon use efficiency in a model soil. Nat. Commun. 11, 3684. https://doi.org/10.1038/s41467-020-17502-z.
Edgar, R.C., 2010. Search and clustering orders of magnitude faster than BLAST. Bioinformatics 26, 2460–2461. https://doi.org/10.1093/bioinformatics/btq461.
Fierer, N., Bradford, M.A., Jackson, R.B., 2007. Toward an ecological classification of soil bacteria. Ecology 88, 1354–1364. https://doi.org/10.1890/05-1839.
García-Angulo, D., Hereş, A.-M., Fernández-López, M., Flores, O., Sanz, M.J., Rey, A., Valladares, F., Curiel Yuste, J., 2020. Holm oak decline and mortality exacerbates drought effects on soil biogeochemical cycling and soil microbial communities across a climatic gradient. Soil Biol. Biochem. 149, 107921. https://doi.org/10.1016/j.soilbio.2020.107921.
Gazol, A., Hereş, A.-M., Curiel Yuste, J., 2021. Land-use practices (coppices and dehesas) and management intensity modulate responses of Holm oak growth to drought. Agric. For. Meteorol. 297, 108235. https://doi.org/10.1016/j.agrformet.2020.108235.
Gleixner, G., 2013. Soil organic matter dynamics: a biological perspective derived from the use of compound-specific isotopes studies. Ecol. Res. 28, 683–695. https://doi.org/10.1007/s11284-012-1022-9.
Graham, E.B., Knelman, J.E., Schindlbacher, A., Siciliano, S., Breulmann, M., Yannarell, A., Beman, J.M., Abell, G., Philippot, L., Prosser, J., Foulquier, A., Yuste, J.C., Glanville, H.C., Jones, D.L., Angel, R., Salminen, J., Newton, R.J., Bürgmann, H., Ingram, L.J., Hamer, U., Siljanen, H.M.P., Peltoniemi, K., Potthast, K., Bañeras, L., Hartmann, M., Banerjee, S., Yu, R.-Q., Nogaro, G., Richter, A., Koranda, M., Castle, S.C., Goberna, M., Song, B., Chatterjee, A., Nunes, O.C., Lopes, A.R., Cao, Y., Kaisermann, A., Hallin, S., Strickland, M.S., Garcia-Pausas, J., Barba, J., Kang, H., Isobe, K., Papaspyrou, S., Pastorelli, R., Lagomarsino, A., Lindström, E.S., Basiliko, N., Nemergut, D.R., 2016. Microbes as engines of ecosystem function: when does community structure enhance predictions of ecosystem processes? Front. Microbiol. 7. https://doi.org/10.3389/fmicb.2016.00214.
Graham, E.B., Wieder, W.R., Leff, J.W., Weintraub, S.R., Townsend, A.R., Cleveland, C. C., Philippot, L., Nemergut, D.R., 2014. Do we need to understand microbial communities to predict ecosystem function? A comparison of statistical models of nitrogen cycling processes. Soil Biol. Biochem. 68, 279–282. https://doi.org/10.1016/j.soilbio.2013.08.023.
Guenet, B., Gabrielle, B., Chenu, C., Arrouays, D., Balesdent, J., Bernoux, M., Bruni, E., Caliman, J., Cardinael, R., Chen, S., Ciais, P., Desbois, D., Fouche, J., Frank, S., Henault, C., Lugato, E., Naipal, V., Nesme, T., Obersteiner, M., Pellerin, S., Powlson, D.S., Rasse, D.P., Rees, F., Soussana, J., Su, Y., Tian, H., Valin, H., Zhou, F., 2021. Can N_2O emissions offset the benefits from soil organic carbon storage? Glob. Chang. Biol. 27, 237–256. https://doi.org/10.1111/gcb.15342.
Hall, E.K., Bernhardt, E.S., Bier, R.L., Bradford, M.A., Boot, C.M., Cotner, J.B., Del Giorgio, P.A., Evans, S.E., Graham, E.B., Jones, S.E., Lennon, J.T., Locey, K.J., Nemergut, D., Osborne, B.B., Rocca, J.D., Schimel, J.P., Waldrop, M.P., Wallenstein, M.D., 2018. Understanding how microbiomes influence the systems they inhabit. Nat. Microbiol. 3, 977–982. https://doi.org/10.1038/s41564-018-0201-z.
Harden, T., Jobbgensen, R.G., Meyer', B., Wolti, V., 1993. And substrate-induced respiration in two pesticide-treated soils. Soil Biol. Biochem. 25, 679–683.
Hartman, W.H., Richardson, C.J., 2013. Differential nutrient limitation of soil microbial biomass and metabolic quotients (qCO2): is there a biological stoichiometry of soil microbes? PLoS One 8, e57127. https://doi.org/10.1371/journal.pone.0057127.
Herguido Sevillano, E., Lavado Contador, J.F., Pulido, M., Schnabel, S., 2017. Spatial patterns of lost and remaining trees in the Iberian wooded rangelands. Appl. Geogr. 87, 170–183. https://doi.org/10.1016/j.apgeog.2017.08.011.
Hoffman, M.D., Gelman, A., 2014. The no-U-turn sampler: adaptively setting path lengths in Hamiltonian Monte Carlo. J. Mach. Learn. Res. 15, 1593–1623.
Hollander, M., Wolfe, D.A., 1973. Nonparametric Statistical Methods. John Wiley & Sons, New York.
Kallenbach, C.M., Frey, S.D., Grandy, A.S., 2016. Direct evidence for microbial-derived soil organic matter formation and its ecophysiological controls. Nat. Commun. 7, 13630. https://doi.org/10.1038/ncomms13630.
Khurana, S., Abramoff, R., Bruni, E., Dondini, M., Tupek, B., Guenet, B., Lehtonen, A., Manzoni, S., 2023. Interactive effects of microbial functional diversity and carbon availability on decomposition – A theoretical exploration. Ecol. Model. 486, 110507. https://doi.org/10.1016/j.ecolmodel.2023.110507.
Koch, A.L., 2001. Oligotrophs versus copiotrophs. Bioessays 23, 657–661. https://doi.org/10.1002/bies.1091.
Le Noë, J., Manzoni, S., Abramoff, R., Bölscher, T., Bruni, E., Cardinael, R., Ciais, P., Chenu, C., Clivot, H., Derrien, D., 2023. Soil organic carbon models need independent time-series validation for reliable prediction. Commun. Earth Environ. 4, 158.
Lennon, J.T., Abramoff, R.Z., Allison, S.D., Burckhardt, R.M., DeAngelis, K.M., Dunne, J. P., Frey, S.D., Friedlingstein, P., Hawkes, C.V., Hungate, B.A., Khurana, S., Kivlin, S. N., Levine, N.M., Manzoni, S., Martiny, A.C., Martiny, J.B.H., Nguyen, N.K., Rawat, M., Talmy, D., Todd-Brown, K., Vogt, M., Wieder, W.R., Zakem, E.J., 2024. Priorities, opportunities, and challenges for integrating microorganisms into earth system models for climate change prediction. mBio 15, e00455–e00524. https://doi.org/10.1128/mbio.00455-24.
Levene, H., 1960. Contributions to Probability and Statistics, I, Olkin. ed. Stanford University Press, Palo Alto.
Li, Z., Tian, D., Wang, B., Wang, J., Wang, S., Chen, H.Y.H., Xu, X., Wang, C., He, N., Niu, S., 2019. Microbes drive global soil nitrogen mineralization and availability. Glob. Chang. Biol. 25, 1078–1088. https://doi.org/10.1111/gcb.14557.
Li, Zhen, William J. Riley, Gianna L. Marschmann, Ulas Karaoz, Ian A. Shirley, Qiong Wu, Nicholas J. Bouskill, et al. "A Framework for Integrating Genomics, Microbial Traits, and Ecosystem Biogeochemistry." Nature Communications 16, no. 1 (March 4, 2025): 2186. doi: 10.1038/s41467-025-57386-5.
Loreau, M., 2001. Microbial diversity, producer-decomposer interactions and ecosystem processes: a theoretical model. Proc. R. Soc. Lond. Ser. B-Biol. Sci. 268, 303–309.
Louis, B.P., Maron, P.-A., Viaud, V., Leterme, P., Menasseri-Aubry, S., 2016. Soil C and N models that integrate microbial diversity. Environ. Chem. Lett. 14, 331–344. https://doi.org/10.1007/s10311-016-0571-5.
Luo, Y., Weng, E., Wu, X., Gao, C., Zhou, X., Zhang, L., 2009. Parameter identifiability, constraint, and equifinality in data assimilation with ecosystem models. Ecol. Appl. 19, 571–574. https://doi.org/10.1890/08-0561.1.
Mäkipää, R., 2023. How does management affect soil C sequestration and greenhouse gas fluxes in boreal and temperate forests? – A review. For. Ecol. Manage.
Malik, A.A., Martiny, J.B.H., Brodie, E.L., Martiny, A.C., Treseder, K.K., Allison, S.D., 2020. Defining trait-based microbial strategies with consequences for soil carbon cycling under climate change. ISME J. 14, 1–9. https://doi.org/10.1038/s41396-019-0510-0.
Malik, A.A., Puissant, J., Buckeridge, K.M., Goodall, T., Jehmlich, N., Chowdhury, S., Gweon, H.S., Peyton, J.M., Mason, K.E., Van Agtmaal, M., Blaud, A., Clark, I.M., Whitaker, J., Pywell, R.F., Ostle, N., Gleixner, G., Griffiths, R.I., 2018. Land use driven change in soil pH affects microbial carbon cycling processes. Nat. Commun. 9, 3591. https://doi.org/10.1038/s41467-018-05980-1.
Mambelli, S., Bird, J.A., Gleixner, G., Dawson, T.E., Torn, M.S., 2011. Relative contribution of foliar and fine root pine litter to the molecular composition of soil organic matter after in situ degradation. S0146638011001653 Org Geochem.. https://doi.org/10.1016/j.orggeochem.2011.06.008.
Manzoni, S., Porporato, A., 2009. Soil carbon and nitrogen mineralization: Theory and models across scales. Soil Biol. Biochem. 41, 1355–1379. https://doi.org/10.1016/j.soilbio.2009.02.031.
Manzoni, S., Porporato, A., 2007. Theoretical analysis of nonlinearities and feedbacks in soil carbon and nitrogen cycles. Soil Biol. Biochem. 39, 1542–1556.
Manzoni, S., Schimel, J.P., 2024. Advances in modelling soil microbial dynamics. Soil Biol. Biochem. 197, 109535. https://doi.org/10.1016/j.soilbio.2024.109535.
Manzoni, S., Trofymow, J.A., Jackson, R.B., Porporato, A., 2010. Stoichiometric controls dynamics on carbon, nitrogen, and phosphorus in decomposing litter. Ecol. Monogr. 80, 89–106.
Martiny, J.B.H., Jones, S.E., Lennon, J.T., Martiny, A.C., 2015. Microbiomes in light of traits: a phylogenetic perspective. Science 350, aac9323. https://doi.org/10.1126/science.aac9323.
Maynard, D.S., Crowther, T.W., Bradford, M.A., 2017. Fungal interactions reduce carbon use efficiency. Ecol. Lett. 20, 1034–1042. https://doi.org/10.1111/ele.12801.
McMurdie, P.J., Holmes, S., 2013. phyloseq: an R package for reproducible interactive analysis and graphics of microbiome census data. PLoS One 8, e61217. https://doi.org/10.1371/journal.pone.0061217.
Miller, R.G., 1981. Simultaneous Statistical Inference, 2nd ed. Springer-Verlag, New York.
Nannipieri, P., Ascher, J., Ceccherini, M.T., Landi, L., Pietramellara, G., Renella, G., 2017. Microbial diversity and soil functions. Eur. J. Soil Sci. 68, 12–26. https://doi.org/10.1111/ejss.4_12398.
Nielsen, U.N., Ayres, E., Wall, D.H., Bardgett, R.D., 2011. Soil biodiversity and carbon cycling: a review and synthesis of studies examining diversity–function relationships. Eur. J. Soil Sci. 62, 105–116. https://doi.org/10.1111/j.1365-2389.2010.01314.x.
Nilsson, R.H., Larsson, K.-H., Taylor, A.F.S., Bengtsson-Palme, J., Jeppesen, T.S., Schigel, D., Kennedy, P., Picard, K., Glöckner, F.O., Tedersoo, L., Saar, I., Kõljalg, U., Abarenkov, K., 2019. The UNITE database for molecular identification of fungi: handling dark taxa and parallel taxonomic classifications. Nucleic Acids Res. 47, D259–D264. https://doi.org/10.1093/nar/gky1022.
Parton, W.J., Stewart, J.W.B., Cole, C.V., 1988. Dynamics of C, N, P and S in grassland soils: a model. Biogeochemistry 5, 109–131. https://doi.org/10.1007/BF02180320.
Paul, E., 2007. Soil Microbiology, Ecology and Biogeochemistry. Academic Press, San Diego, CA, USA.
Pennekamp, F., Pontarp, M., Tabi, A., Altermatt, F., Alther, R., Choffat, Y., Fronhofer, E. A., Ganesanandamoorthy, P., Garnier, A., Griffiths, J.I., Greene, S., Horgan, K., Massie, T.M., Mächler, E., Palamara, G.M., Seymour, M., Petchey, O.L., 2018. Biodiversity increases and decreases ecosystem stability. Nature 563, 109–112. https://doi.org/10.1038/s41586-018-0627-8.
Põlme, S., Abarenkov, K., Henrik Nilsson, R., Lindahl, B.D., Clemmensen, K.E., Kauserud, H., Nguyen, N., Kjøller, R., Bates, S.T., Baldrian, P., Frøslev, T.G., Adojaan, K., Vizzini, A., Suija, A., Pfister, D., Baral, H.-O., Järv, H., Madrid, H., Nordén, J., Liu, J.-K., Pawlowska, J., Põldmaa, K., Pärtel, K., Runnel, K., Hansen, K., Larsson, K.-H., Hyde, K.D., Sandoval-Denis, M., Smith, M.E., Toome-Heller, M., Wijayawardene, N.N., Menolli, N., Reynolds, N.K., Drenkhan, R., Maharachchikumbura, S.S.N., Gibertoni, T.B., Læssøe, T., Davis, W., Tokarev, Y., Corrales, A., Soares, A.M., Agan, A., Machado, A.R., Argüelles-Moyao, A., Detheridge, A., De Meiras-Ottoni, A., Verbeken, A., Dutta, A.K., Cui, B.-K.,

Pradeep, C.K., Marín, C., Stanton, D., Gohar, D., Wanasinghe, D.N., Otsing, E., Aslani, F., Griffith, G.W., Lumbsch, T.H., Grossart, H.-P., Masigol, H., Timling, I., Hiiesalu, I., Oja, J., Kupagme, J.Y., Geml, J., Alvarez-Manjarrez, J., Ilves, K., Loit, K., Adamson, K., Nara, K., Küngas, K., Rojas-Jimenez, K., Bitenieks, K., Irinyi, L., Nagy, L.G., Soonvald, L., Zhou, L.-W., Wagner, L., Aime, M.C., Öpik, M., Mujica, M.I., Metsoja, M., Ryberg, M., Vasar, M., Murata, M., Nelsen, M.P., Cleary, M., Samarakoon, M.C., Doilom, M., Bahram, M., Hagh-Doust, N., Dulya, O., Johnston, P., Kohout, P., Chen, Q., Tian, Q., Nandi, R., Amiri, R., Perera, R.H., Dos Santos Chikowski, R., Mendes-Alvarenga, R.L., Garibay-Orijel, R., Gielen, R., Phookamsak, R., Jayawardena, R.S., Rahimlou, S., Karunarathna, S.C., Tibpromma, S., Brown, S.P., Sepp, S.-K., Mundra, S., Luo, Z.-H., Bose, T., Vahter, T., Netherway, T., Yang, T., May, T., Varga, T., Li, W., Coimbra, V.R.M., De Oliveira, V. R.T., De Lima, V.X., Mikryukov, V.S., Lu, Y., Matsuda, Y., Miyamoto, Y., Kõljalg, U., Tedersoo, L., 2021. Correction to: FungalTraits: a user friendly traits database of fungi and fungus-like stramenopiles. Fungal Divers. 107, 129–132. https://doi.org/10.1007/s13225-021-00470-0.

Pulido, F.J., Díaz, JM., Hidalgo De Trucios, S.J., 2001. Size structure and regeneration of Spanish holm oak Quercus ilex forests and dehesas: effects of agroforestry use on their long-term sustainability. For. Ecol. Manage. 146, 1–13. https://doi.org/10.1016/S0378-1127(00)00443-6.

R Core Team, 2022. R: A language and environment for statistical computing.

Robertson, A.D., Paustian, K., Ogle, S., Wallenstein, M.D., Lugato, E., Cotrufo, M.F., 2019. Unifying soil organic matter formation and persistence frameworks: the MEMS model. Biogeosciences 16, 1225–1248. https://doi.org/10.5194/bg-16-1225-2019.

Royston, J.P., 1982. An extension of Shapiro and Wilk's W test for normality to large samples. Appl. Stat. 31, 115. https://doi.org/10.2307/2347973.

Rubino, M., Dungait, J.A.J., Evershed, R.P., Bertolini, T., De Angelis, P., D'Onofrio, A., Lagomarsino, A., Lubritto, C., Merola, A., Terrasi, F., 2010. Carbon input belowground is the major C flux contributing to leaf litter mass loss: Evidences from a 13C labelled-leaf litter experiment. Soil Biol. Biochem. 42, 1009–1016. https://doi.org/10.1016/j.soilbio.2010.02.018.

Sahu, P.K., Singh, D.P., Prabha, R., Meena, K.K., Abhilash, P.C., 2019. Connecting microbial capabilities with the soil and plant health: Options for agricultural sustainability. Ecol. Ind. 105, 601–612. https://doi.org/10.1016/j.ecolind.2018.05.084.

Saifuddin, M., Abramoff, R.Z., Davidson, E.A., Dietze, M.C., Finzi, A.C., 2021. Identifying data needed to reduce parameter uncertainty in a coupled microbial soil C and N decomposition model. J. Geophys. Res. Biogeo. 126, e2021JG006593. https://doi.org/10.1029/2021JG006593.

Setälä, H., McLean, M.A., 2004. Decomposition rate of organic substrates in relation to the species diversity of soil saprophytic fungi. Oecologia 139, 98–107. https://doi.org/10.1007/s00442-003-1478-y.

Shi, Z., Crowell, S., Luo, Y., Moore, B., 2018. Model structures amplify uncertainty in predicted soil carbon responses to climate change. Nat. Commun. 9, 2171. https://doi.org/10.1038/s41467-018-04526-9.

Soares, M., Kritzberg, E.S., Rousk, J., 2017. Labile carbon 'primes' fungal use of nitrogen from submerged leaf litter. FEMS Microbiol. Ecol. 93. https://doi.org/10.1093/femsec/fix110.

Soetaert, K., Petzoldt, T., 2010. Inverse modelling, sensitivity and Monte Carlo analysis in R using package FME. J. Stat. Softw. 33, 1–28. https://doi.org/10.18637/jss.v033.i03.

Stan Development Team, 2024. Stan: A C++ Library for Probability and Sampling, Version 2.32.0.

Sterner, R.W., Elser, J.J., 2002. Ecological stoichiometry. The biology of elements from molecules to the biosphere. Princeton University Press, Princeton and Oxford.

Sulman, B.N., Phillips, R.P., Oishi, A.C., Shevliakova, E., Pacala, S.W., 2014. Microbe-driven turnover offsets mineral-mediated storage of soil carbon under elevated CO2. Nat. Clim. Chang. 4, 1099–1102. https://doi.org/10.1038/nclimate2436.

Tang, J.Y., Riley, W.J., 2017. SUPECA kinetics for scaling redox reactions in networks of mixed substrates and consumers and an example application to aerobic soil respiration. Geosci. Model Dev. 10, 3277–3295. https://doi.org/10.5194/gmd-10-3277-2017.

Tate, K.R., 2017. Microbial Biomass: A Paradigm Shift in Terrestrial Biogeochemistry. World Scientific Publishing Europe Ltd., London, United Kingdom.

Tiunov, A.V., Scheu, S., 2005. Facilitative interactions rather than resource partitioning drive diversity-functioning relationships in laboratory fungal communities. Ecol. Lett. 8, 618–625. https://doi.org/10.1111/j.1461-0248.2005.00757.x.

Todd-Brown, K.E.O., Randerson, J.T., Hopkins, F., Arora, V., Hajima, T., Jones, C., Shevliakova, E., Tjiputra, J., Volodin, E., Wu, T., Zhang, Q., Allison, S.D., 2014. Changes in soil organic carbon storage predicted by Earth system models during the 21st century. Biogeosciences 11, 2341–2356. https://doi.org/10.5194/bg-11-2341-2014.

Valentin, L., Rajala, T., Peltoniemi, M., Heinonsalo, J., Pennanen, T., Mäkipää, R., 2014. Loss of diversity in wood-inhabiting fungal communities affects decomposition activity in Norway spruce wood. Front. Microbiol. 5. https://doi.org/10.3389/fmicb.2014.00230.

Wang, C., Wang, X., Zhang, Y., Morrissey, E., Liu, Y., Sun, L., Qu, L., Sang, C., Zhang, H., Li, G., Zhang, L., Fang, Y., 2023. Integrating microbial community properties, biomass and necromass to predict cropland soil organic carbon. ISME Commun. 3, 86. https://doi.org/10.1038/s43705-023-00300-1.

Wang, G., Jagadamma, S., Mayes, M.A., Schadt, C.W., Megan Steinweg, J., Gu, L., Post, W.M., 2015. Microbial dormancy improves development and experimental validation of ecosystem model. ISME J. 9, 226–237. https://doi.org/10.1038/ismej.2014.120.

Wieder, W.R., Grandy, A.S., Kallenbach, C.M., Bonan, G.B., 2014. Integrating microbial physiology and physio-chemical principles in soils with the MIcrobial-MIneral Carbon Stabilization (MIMICS) model. Biogeosciences 11, 3899–3917. https://doi.org/10.5194/bg-11-3899-2014.

Wieder, W.R., Grandy, A.S., Kallenbach, C.M., Taylor, P.G., Bonan, G.B., 2015. Representing life in the Earth system with soil microbial functional traits in the MIMICS model. Geosci. Model Dev. 8, 1789–1808. https://doi.org/10.5194/gmd-8-1789-2015.

Wilkinson, A., Solan, M., Alexander, I., Johnson, D., 2012. Species richness and nitrogen supply regulate the productivity and respiration of ectomycorrhizal fungi in pure culture. Fungal Ecol. 5, 211–222. https://doi.org/10.1016/j.funeco.2011.08.007.

Wohl, D.L., Arora, S., Gladstone, J.R., 2004. Functional redundancy supports biodiversity and ecosystem function in a closed and constant environment. Ecology 85, 1534–1540. https://doi.org/10.1890/03-3050.

Xu, X., Schimel, J.P., Janssens, I.A., Song, X., Song, C., Yu, G., Sinsabaugh, R.L., Tang, D., Zhang, X., Thornton, Peter, E., 2017. Global pattern and controls of soil microbial metabolic quotient. Ecol. Monogr. 87, 429–441. https://doi.org/10.1002/ecm.1258.

Xu, X., Thornton, P.E., Post, W.M., 2013. A global analysis of soil microbial biomass carbon, nitrogen and phosphorus in terrestrial ecosystems. Glob. Ecol. Biogeogr. 22, 737–749. https://doi.org/10.1111/geb.12029.

Zhang, Y., Lavallee, J.M., Robertson, A.D., Even, R., Ogle, S.M., Paustian, K., Cotrufo, M. F., 2021. Simulating measurable ecosystem carbon and nitrogen dynamics with the mechanistically defined MEMS 2.0 model. Biogeosciences 18, 3147–3171. https://doi.org/10.5194/bg-18-3147-2021.